Error-Covariance Reset in the Multiplicative Extended Kalman Filter for Attitude Estimation

Article *in* Journal of Guidance, Control, and Dynamics · July 2023

DOI: 10.2514/1.G007653

CITATIONS
3

READS
1,276

4 authors, including:

Landis Markley
retired
178 PUBLICATIONS **10,473** CITATIONS
SEE PROFILE

John Crassidis
University at Buffalo, State University of New York
274 PUBLICATIONS **11,413** CITATIONS
SEE PROFILE

Error-Covariance Reset in the Multiplicative Extended Kalman Filter for Attitude Estimation *

F. Landis Markley†

Yang Cheng‡
XAnalytix Systems, LLC, Clarence Center, NY 14032-9136

John L. Crassidis§
University at Buffalo, State University of New York, Amherst, NY, 14260-4400

Reid G. Reynolds¶
Millennium Space Systems, El Segundo, California 90245

This paper presents a study of the reset step in the multiplicative extended Kalman filter (MEKF). This filter is widely used for spacecraft attitude estimation, which typically involves estimating the attitude and gyro drift in real time using external sensors such as star trackers. The basic idea of the MEKF is to use the quaternion or direction-cosine matrix as the "global" attitude parameterization and a three-component state vector for the "local" parameterization of attitude errors. The true attitude is expressed as the product of the error attitude and the estimate rather than as the sum of the error and the estimate. The reset operation moves the local error to the global variable. This reset does not add new information, but it changes the reference frame for the attitude error-covariance. This results in an error-covariance reset that is very different from the measurement update of the error-covariance in the MEKF. The effects of using an error-covariance reset in the MEKF are analyzed in this work. The results from this work can be applied to any application involving attitude estimation as part of its process, such as inertial navigation.

I. Introduction

Attitude estimation refers to the process of estimating the current attitude state of a system from a set of measured observations. This state estimation problem involves finding the best estimate of the true system state using a dynamic model and measurements that are both corrupted with random noise of known statistics. The variables to be estimated are usually collected into a state vector, which typically includes other variables in addition to the attitude. For example,

*Presented at 2022 AAS/AIAA Astrodynamics Specialist Conference, Charlotte, NC, August 7–11 2022.

†Deceased, December 5, 2021.

‡Senior Engineer. Associate Fellow AIAA. Email: yang.cheng@xanalytixsystems.com

§SUNY Distinguished Professor and Moog Endowed Chaired Professor of Innovation, Department of Mechanical & Aerospace Engineering. Fellow AIAA. Email: johnc@buffalo.edu.

¶Principal Guidance Navigation and Control Engineer. Senior Member AIAA. Email: reid.reynolds@millennium-space.com.

for spacecraft applications, attitude sensor measurements, such as those provided by a star tracker, can be combined with an attitude kinematics model, which is propagated using gyro measurements [1]. For inertial navigation applications, external sensor measurements, such as those provided by a Global Navigation Satellite System, can be combined with an attitude/position kinematics model, which is propagated using measurements from inertial measurement units (IMUs), typically including both gyros and accelerometers [2]. However, all IMU sensors have inherent drift, or bias, which causes inaccuracies in the propagated model. A complementary filter is used to simultaneously estimate the attitude and IMU drift from the measurements.

The extended Kalman filter [3] (EKF) is the workhorse of real-time spacecraft attitude estimation. Since the group SO(3) of rotation matrices has dimension three, most attitude estimation EKFs use lower-dimensional attitude parameterizations than the nine-parameter attitude matrix itself. The fact that all three-parameter parameterizations of SO(3) are singular or discontinuous for certain attitudes [4] has led to extended discussions of constraints and attitude parameterizations in EKFs [5–9]. These issues are now well understood, however, and the EKF, especially in the form known as the multiplicative extended Kalman filter (MEKF) [5, 6, 10], has performed admirably in the vast majority of attitude estimation applications [1].

In the standard MEKF the global parameterization is given by the quaternion [11] while the local attitude-error parameterization is given by a three-component vector that can easily be related to small roll, pitch and yaw attitude errors. The quaternion is chosen because it has no singularities, but it must obey a unit-norm constraint. This is usually done by a brute-force method, which is valid to within the usual first-order error assumptions in the EKF. The direction-cosine matrix can be used for the global attitude, but the "closest" orthogonal matrix must then be found to maintain orthogonality in the SO(3) group, which usually involves computationally expensive routines involving the singular value decomposition of a 3×3 matrix. The same advantage of using the quaternion over the direction-cosine matrix applies during the propagation stage of the MEKF; usually a brute-force normalization of the quaternion is sufficient after each time step to overcome numerical errors that can violate the unit-norm constraint.

In the MEKF the true attitude is expressed as the product of the error-attitude and the estimate rather than as the sum of the error and the estimate. The MEKF incorporates a conventional EKF that provides an unconstrained and unbiased estimate of the nonzero expectation of the attitude error. A reset operation moves this update into this global variable. The reset does not add new information, but it changes the reference frame for the attitude error-covariance. This results in an error-covariance reset that is very different from the measurement update of the error-covariance in the EKF. The measurement update of the error-covariance depends only on the assumed statistics of the measurements, but the reset depends on the actual update, which depends on the actual measurements. Some argue against the reset on the grounds that the error-covariance should depend only on the assumed statistics of the measurements [12], but others argue in favor of an error-covariance reset [13–17]. Specifically, a geometric view of the attitude error-covariance reset is provided [13]: the attitude error-covariance is defined in the tangent space of the unit quaternion manifold. The

measurement update still leaves the updated error-covariance in the tangent space of the pre-update quaternion, and it must be mapped to that of the post-update quaternion.

Other state estimation approaches use the full quaternion within the standard additive EKF framework. At least four methods have been proposed to deal with additive quaternion filtering [12]. One involves a brute-force re-normalization of the quaternion after the update stage. Another is to modify the Kalman filter update equations to enforce the norm constraint by means of a Lagrange multiplier [15]. However, these two approaches both yield biased estimates of the quaternion. The third approach involves not enforcing the quaternion norm, and to define the attitude matrix by the dividing the attitude matrix by the norm-square of the un-normalized quaternion. This is called the ray representation, because any quaternion along a ray through the origin corresponds to the same attitude matrix [12]. This approach avoids the complications arising from enforcing the norm constraint, but introduces an unobservable degree of freedom, the quaternion norm. Still, successful implementations of this approach have been achieved, e.g. see [18]. The third approach involves not enforcing the quaternion norm, i.e. without dividing the attitude matrix by the norm-square of the un-normalized quaternion. The attitude matrix is not orthogonal in this case, and the approach can lead to an ill-conditioned error-covariance matrix [9]. None of these approaches require a reset operation, but the MEKF provides many advantages over them, such as giving a direct physical interpretation of the roll, pitch and yaw angle-errors from the error-covariance matrix.

This paper studies the effects of applying an error-covariance reset in the MEKF. This will be done through detailed analytical derivations and numerical simulations. Many different error-parameterizations can be used for the error-vector. The choice of parameterization is to some extent arbitrary. Several will be considered, including the Rodrigues-Gibbs vector, the vector part of the quaternion, the modified Rodrigues parameter vector, and the rotation vector. The error-covariance reset will differ for the different parameterizations, but it has been determined that almost all the resets are the same to first order in error-vector.

The organization of this paper is as follows. First, a review of the attitude parameterizations used in this work is shown. Then, the basic concept of the MEKF is given, followed by showing the main equations used for the attitude error-covariance reset. Next, various parameterizations, including the Rodrigues-Gibbs vector, vector part of the quaternion, the modified Rodrigues parameter vector, and rotation vector, to parameterize the local attitude errors are shown. Analytical test cases are then shown. This is followed by the implementation approach for the attitude error-covariance reset operation in the Kalman and Unscented filters. Finally, numerical simulations are provided to show the performance characteristics for both the Kalman and Unscented filters.

II. Attitude Parameterizations

This section presents a brief review of the attitude parameterizations used throughout this paper. See [12] for more details. The attitude matrix A, often referred to as the direction cosine matrix or rotation matrix, maps one frame to

another. The attitude matrix is an orthogonal matrix, i.e. its inverse is given by its transpose with $AA^T = A^TA = I_3$ where I_3 is a 3×3 identity matrix, and proper, i.e. its determinant is +1.

A quaternion $\boldsymbol{q}$ has a three-vector part $\boldsymbol{q}_{1:3}$ and a scalar part q_4:

$$\boldsymbol{q} = \begin{bmatrix} \boldsymbol{q}_{1:3} \\ q_4 \end{bmatrix}, \quad \text{where} \quad \boldsymbol{q}_{1:3} = \begin{bmatrix} q_1 \\ q_2 \\ q_3 \end{bmatrix} \tag{1}$$

Also, $\boldsymbol{q}_{1:3} = \boldsymbol{e}\sin(\vartheta/2)$ and $q_4 = \cos(\vartheta/2)$, where $\boldsymbol{e}$ is the unit Euler axis and ϑ is the rotation angle. The attitude matrix is related to the quaternion by

$$\begin{aligned} A(\boldsymbol{q}) &= \left(q_4^2 - ||\boldsymbol{q}_{1:3}||^2\right) I_3 + 2\boldsymbol{q}_{1:3}\boldsymbol{q}_{1:3}^T - 2q_4[\boldsymbol{q}_{1:3}\times] \\ &= \Xi^T(\boldsymbol{q})\Psi(\boldsymbol{q}) \end{aligned} \tag{2}$$

where

$$\Xi(\boldsymbol{q}) \equiv \begin{bmatrix} q_4 I_3 + [\boldsymbol{q}_{1:3}\times] \\ -\boldsymbol{q}_{1:3}^T \end{bmatrix} \tag{3a}$$

$$\Psi(\boldsymbol{q}) \equiv \begin{bmatrix} q_4 I_3 - [\boldsymbol{q}_{1:3}\times] \\ -\boldsymbol{q}_{1:3}^T \end{bmatrix} \tag{3b}$$

Also, $[\boldsymbol{q}_{1:3}\times]$ is the cross-product matrix defined by

$$[\boldsymbol{q}_{1:3}\times] \equiv \begin{bmatrix} 0 & -q_3 & q_2 \\ q_3 & 0 & -q_1 \\ -q_2 & q_1 & 0 \end{bmatrix} \tag{4}$$

For small angles the vector part of the quaternion is approximately equal to half angles [11], where these small angles are denoted by the vector $\boldsymbol{\delta}$. For small angle-rotations the attitude matrix can be approximated by $A(\boldsymbol{\delta}) = I_3 - [\boldsymbol{\delta}\times]$. Quaternion multiplication of a pair of quaternions, $\bar{\boldsymbol{q}}$ and $\boldsymbol{q}$, is given by

$$\bar{\boldsymbol{q}} \otimes \boldsymbol{q} = \begin{bmatrix} q_4\,\bar{\boldsymbol{q}}_{1:3} + \bar{q}_4\,\boldsymbol{q}_{1:3} - \bar{\boldsymbol{q}}_{1:3} \times \boldsymbol{q}_{1:3} \\ \bar{q}_4\,q_4 - \bar{\boldsymbol{q}}_{1:3} \cdot \boldsymbol{q}_{1:3} \end{bmatrix} \tag{5}$$

Also, the quaternion multiplication in Eq. (5) can be written as $\bar{\boldsymbol{q}} \otimes \boldsymbol{q} = [\Psi(\bar{\boldsymbol{q}}) \;\; \bar{\boldsymbol{q}}]\boldsymbol{q} = [\Xi(\boldsymbol{q}) \;\; \boldsymbol{q}]\bar{\boldsymbol{q}}$. Here the convention of [11] is adopted, where the quaternions are multiplied in the same order as the attitude matrix multiplication, in contrast to the usual convention established by Hamilton. Thus, $A(\bar{\boldsymbol{q}})A(\boldsymbol{q}) = A(\bar{\boldsymbol{q}} \otimes \boldsymbol{q})$. The inverse quaternion is denoted by $\boldsymbol{q}^{-1} \equiv [-\boldsymbol{q}_{1:3}^T \;\; q_4]^T$, which gives $A(\boldsymbol{q}^{-1} \otimes \boldsymbol{q}) = A(\boldsymbol{q} \otimes \boldsymbol{q}^{-1}) = I_3$.

The attitude matrix parameterized by the Euler axis and angle is given by

$$\begin{aligned} A(\boldsymbol{e}, \vartheta) &= \cos\vartheta \, I_3 - \sin\vartheta [\boldsymbol{e}\times] + (1 - \cos\vartheta)\boldsymbol{e}\boldsymbol{e}^T \\ &= I_3 - \sin\vartheta [\boldsymbol{e}\times] + (1 - \cos\vartheta)[\boldsymbol{e}\times]^2 \end{aligned} \tag{6}$$

It is often convenient for analysis to combine the Euler axis and angle into a three-component vector:

$$\boldsymbol{\vartheta} \equiv \vartheta \, \boldsymbol{e} \tag{7}$$

The attitude matrix parameterized by this rotation vector is given by

$$A(\boldsymbol{\vartheta}) = \exp\left(-[\boldsymbol{\vartheta}\times]\right) \tag{8}$$

where exp is the matrix exponential.

The three Rodrigues parameters made their appearance in Rodrigues' classic 1840 paper [12]. They were later represented as the "vector semitangent of version" by J. Willard Gibbs, who invented modern vector notation. For this reason, the vector of Rodrigues parameters is often called the Gibbs vector, or Rodrigues-Gibbs vector, and denoted by $\boldsymbol{g}$. This parameterization is related to the quaternion by

$$\boldsymbol{g} = \frac{\boldsymbol{q}_{1:3}}{q_4} \tag{9}$$

which has the inverse

$$\boldsymbol{q} = \frac{\pm 1}{\sqrt{1 + \|\boldsymbol{g}\|^2}} \begin{bmatrix} \boldsymbol{g} \\ 1 \end{bmatrix} \tag{10}$$

The Rodrigues-Gibbs vector in terms of the Euler axis and angle is given by

$$\boldsymbol{g}(\boldsymbol{e}, \vartheta) = \boldsymbol{e} \tan(\vartheta/2) \tag{11}$$

The attitude matrix parameterized by the Rodrigues-Gibbs vector is given by

$$\begin{aligned} A(\boldsymbol{g}) &= \frac{(1 - \|\boldsymbol{g}\|^2) I_3 - 2[\boldsymbol{g}\times] + 2\,\boldsymbol{g}\,\boldsymbol{g}^T}{1 + \|\boldsymbol{g}\|^2} \\ &= I_3 + 2\frac{[\boldsymbol{g}\times]^2 - [\boldsymbol{g}\times]}{1 + \|\boldsymbol{g}\|^2} \end{aligned} \tag{12}$$

The Rodrigues-Gibbs vector corresponding to the quaternion product $\bar{\bar{\boldsymbol{q}}} = \bar{\boldsymbol{q}} \otimes \boldsymbol{q}$ is

$$\bar{\bar{\boldsymbol{g}}} = \frac{\bar{\boldsymbol{g}} + \boldsymbol{g} - \bar{\boldsymbol{g}} \times \boldsymbol{g}}{1 - \bar{\boldsymbol{g}} \cdot \boldsymbol{g}} \tag{13}$$

This is not a bilinear function of the constituent Rodrigues-Gibbs vectors, so it cannot be represented as a matrix product like the quaternion composition.

The modified Rodrigues parameter (MRP) vector is related to the quaternion by

$$\boldsymbol{p} = \frac{\boldsymbol{q}_{1:3}}{1 + q_4} \tag{14}$$

which has the inverse

$$\boldsymbol{q} = \frac{1}{1 + \|\boldsymbol{p}\|^2} \begin{bmatrix} 2\boldsymbol{p} \\ 1 - \|\boldsymbol{p}\|^2 \end{bmatrix} \tag{15}$$

The MRP vector in terms of the Euler axis and angle is given by

$$\boldsymbol{p}(\boldsymbol{e}, \vartheta) = \boldsymbol{e} \tan(\vartheta/4) \tag{16}$$

The attitude matrix parameterized by the MRP vector is given by

$$\begin{aligned} A(\boldsymbol{p}) &= \left(\frac{I_3 - [\boldsymbol{p}\times]}{I_3 + [\boldsymbol{p}\times]}\right)^2 \\ &= I_3 + \frac{8\,[\boldsymbol{p}\times]^2 - 4\left(1 - \|\boldsymbol{p}\|^2\right)[\boldsymbol{p}\times]}{(1 + \|\boldsymbol{p}\|^2)^2} \end{aligned} \tag{17}$$

The MRP vector corresponding to the quaternion product $\bar{\bar{\boldsymbol{q}}} = \bar{\boldsymbol{q}} \otimes \boldsymbol{q}$ is

$$\bar{\bar{\boldsymbol{p}}} = \frac{\left(1 - \|\boldsymbol{p}\|^2\right)\bar{\boldsymbol{p}} + \left(1 - \|\bar{\boldsymbol{p}}\|^2\right)\boldsymbol{p} - 2\,\bar{\boldsymbol{p}} \times \boldsymbol{p}}{1 + \|\boldsymbol{p}\|^2\|\bar{\boldsymbol{p}}\|^2 - 2\,\bar{\boldsymbol{p}} \cdot \boldsymbol{p}} \tag{18}$$

See [12] for a discussion on other properties of the MRP vector.

III. Multiplicative Extended Kalman Filter

The basic idea of the MEKF is to use the direction cosine matrix or quaternion as the "global" attitude parameterization and a three-component state vector $\boldsymbol{\delta}$ for the "local" parameterization of attitude errors [12]. The true attitude is expressed as the product of the error attitude and the estimate rather than as the sum of the error and the estimate. Using the attitude matrix or direction cosine matrix for the global parameterization gives

$$A = A(\boldsymbol{\delta})\hat{A} \tag{19}$$

where $\hat{}$ denotes the estimated variable, and $A(\boldsymbol{\delta} = \mathbf{0}) = I_3$. The MEKF incorporates a conventional EKF that provides an unconstrained and unbiased estimate of the nonzero expectation $\hat{\boldsymbol{\delta}}$ of the attitude error. A reset operation moves this update into this global variable by

$$\hat{A}^+ = A(\hat{\boldsymbol{\delta}})\hat{A} \tag{20}$$

and sets $\hat{\boldsymbol{\delta}}^+$ to zero, where post-reset quantities are distinguished by the superscript.

IV. Attitude Error-Covariance Reset

The true attitude is not changed by the reset, so Eqs. (19) and (20) give

$$\begin{aligned} A &= A(\boldsymbol{\delta})\hat{A} \\ &= A\left(\boldsymbol{\delta}^+\right)\hat{A}^+ \\ &= A\left(\boldsymbol{\delta}^+\right)A(\hat{\boldsymbol{\delta}})\hat{A} \end{aligned} \tag{21}$$

It follows from this that $A(\boldsymbol{\delta}) = A\left(\boldsymbol{\delta}^+\right)A(\hat{\boldsymbol{\delta}})$ or equivalently

$$A\left(\boldsymbol{\delta}^+\right) = A(\boldsymbol{\delta})\, A^{-1}(\hat{\boldsymbol{\delta}}) \tag{22}$$

The pre-reset and post-reset error-covariances are the covariances of $\boldsymbol{\delta}$ and $\boldsymbol{\delta}^+$, respectively, so Eq. (22), which defines a nonlinear mapping from $\boldsymbol{\delta}$ to $\boldsymbol{\delta}^+$, is the key equation for specifying the error-covariance reset.

Many different error parameterizations can be used for the error vector $\boldsymbol{\delta}$. The choice of parameterization is to some extent arbitrary, and several will be considered. The error-covariance reset will differ for the different parameterizations, but it is found that almost all the resets are the same to first order in $\hat{\boldsymbol{\delta}}$.

A. Rodrigues-Gibbs Vector Attitude Error Parameterization

The parameterization of local attitude errors by the Rodrigues-Gibbs vector, $\boldsymbol{\delta} = \boldsymbol{g} = \boldsymbol{e}\tan(\vartheta/2)$, where $\boldsymbol{e}$ is the Euler axis of rotation and ϑ is the Euler angle of rotation, is first considered. Section 6.2.1.2 of [12] points out several advantages of this parameterization. Some of these advantages are purely computational, but this parameterization also has the conceptual advantage of mapping the rotation group into three-dimensional Euclidean space, with the largest possible 180° attitude errors mapped to points at infinity. Thus, probability distributions with infinitely long tails, such as Gaussian distributions, make sense in this parameter space.

Expressing Eq. (22) in terms of the product rule for the Rodrigues-Gibbs vector from Eq. (13), writing $\boldsymbol{g} = \hat{\boldsymbol{g}} + \boldsymbol{\Delta g}$, where the use of $\boldsymbol{\Delta}$ denotes the estimate error, and expanding in powers of $\boldsymbol{\Delta g}$ gives

$$\begin{aligned}
\boldsymbol{g}^+ &= \frac{\boldsymbol{g} - \hat{\boldsymbol{g}} + \boldsymbol{g}\times\hat{\boldsymbol{g}}}{1 + \boldsymbol{g}\cdot\hat{\boldsymbol{g}}} \\
&= \frac{\boldsymbol{\Delta g} + \boldsymbol{\Delta g}\times\hat{\boldsymbol{g}}}{1 + (\hat{\boldsymbol{g}} + \boldsymbol{\Delta g})\cdot\hat{\boldsymbol{g}}} \\
&= \Gamma_g(\hat{\boldsymbol{g}})\boldsymbol{\Delta g}\left[1 - \frac{\hat{\boldsymbol{g}}\cdot\boldsymbol{\Delta g}}{1 + \|\hat{\boldsymbol{g}}\|^2} + \left(\frac{\hat{\boldsymbol{g}}\cdot\boldsymbol{\Delta g}}{1 + \|\hat{\boldsymbol{g}}\|^2}\right)^2 + \ldots\right]
\end{aligned} \tag{23}$$

with

$$\Gamma_g(\hat{\boldsymbol{g}}) \equiv \frac{I_3 - [\hat{\boldsymbol{g}}\times]}{1 + \|\hat{\boldsymbol{g}}\|^2} \tag{24}$$

Retaining only the lowest-order nonzero terms, the expectation of Eq. (23) is

$$\begin{aligned}
\hat{\boldsymbol{g}}^+ &= -\Gamma_g(\hat{\boldsymbol{g}})E\left\{\boldsymbol{\Delta g}\frac{\hat{\boldsymbol{g}}\cdot\boldsymbol{\Delta g}}{1 + \|\hat{\boldsymbol{g}}\|^2}\right\} \\
&= -\Gamma_g(\hat{\boldsymbol{g}})\frac{E\left\{\boldsymbol{\Delta g}\boldsymbol{\Delta g}^T\right\}\hat{\boldsymbol{g}}}{1 + \|\hat{\boldsymbol{g}}\|^2} \\
&= -\frac{\Gamma_g(\hat{\boldsymbol{g}})P_g\hat{\boldsymbol{g}}}{1 + \|\hat{\boldsymbol{g}}\|^2}
\end{aligned} \tag{25}$$

where $E\{\cdot\}$ denotes expectation and P_g is the pre-reset error-covariance. The first-order term in $\boldsymbol{\Delta g}$ vanishes because $E\{\boldsymbol{\Delta g}\} = \boldsymbol{0}$ by definition. The reset sets $\hat{\boldsymbol{g}}^+$ to zero, as stated below Eq. (20), so consistency requires

$$\left\|\Gamma_g(\hat{\boldsymbol{g}})P_g\hat{\boldsymbol{g}}\right\| \ll 1 + \|\hat{\boldsymbol{g}}\|^2 \tag{26}$$

To fourth order in $\boldsymbol{\Delta g}$, the second moment of $\hat{\boldsymbol{g}}^+$ is

$$E\left[\boldsymbol{g}^+\left(\boldsymbol{g}^+\right)^T\right] = \Gamma_g(\hat{\boldsymbol{g}})E\left\{\boldsymbol{\Delta g}\left[1 - 2\frac{\hat{\boldsymbol{g}}\cdot\boldsymbol{\Delta g}}{1 + \|\hat{\boldsymbol{g}}\|^2} + 3\left(\frac{\hat{\boldsymbol{g}}\cdot\boldsymbol{\Delta g}}{1 + \|\hat{\boldsymbol{g}}\|^2}\right)^2\right]\boldsymbol{\Delta g}^T\right\}\Gamma_g^T(\hat{\boldsymbol{g}}) \tag{27}$$

Assuming the probability distribution of $\boldsymbol{\Delta g}$ to be Gaussian, the expectation of any odd power of $\boldsymbol{\Delta g}$ vanishes, and the

expectation of the fourth-order term obeys Isserlis' Theorem [19]:

$$E\left[(\Delta g)_p(\Delta g)_q(\Delta g)_m(\Delta g)_n\right] = \left(P_g\right)_{pq}\left(P_g\right)_{mn} + \left(P_g\right)_{pm}\left(P_g\right)_{qn} + \left(P_g\right)_{pn}\left(P_g\right)_{qm} \tag{28}$$

For a random vector $\boldsymbol{x}$ with associated covariance P_x, Isserlis' Theorem gives $E\left\{(\boldsymbol{a}^T\boldsymbol{x})^2\boldsymbol{x}\,\boldsymbol{x}^T\right\} = (\boldsymbol{a}^T P_x\,\boldsymbol{a})P_x + 2P_x\,\boldsymbol{a}\,\boldsymbol{a}^T P_x$, where $\boldsymbol{a}$ is any non-random vector [3]. The post-reset error-covariance is

$$\begin{aligned} P_g^+ &= E\left\{\boldsymbol{g}^+\left(\boldsymbol{g}^+\right)^T\right\} - \hat{\boldsymbol{g}}^+\left(\hat{\boldsymbol{g}}^+\right)^T \\ &= \Gamma_g(\hat{\boldsymbol{g}})P_g\Gamma_g^T(\hat{\boldsymbol{g}})\left[1 + \frac{3\hat{\boldsymbol{g}}^T P_g\hat{\boldsymbol{g}}}{\left(1+\|\hat{\boldsymbol{g}}\|^2\right)^2}\right] + 5\hat{\boldsymbol{g}}^+\left(\hat{\boldsymbol{g}}^+\right)^T \end{aligned} \tag{29}$$

Thus, in addition to satisfying Eq. (26), if the following condition is met:

$$3\hat{\boldsymbol{g}}^T P_g\hat{\boldsymbol{g}} \ll \left(1+\|\hat{\boldsymbol{g}}\|^2\right)^2 \tag{30}$$

then the error-covariance reset will be given to a good approximation by $P_g^+ = \Gamma_g(\hat{\boldsymbol{g}})P_g\Gamma_g^T(\hat{\boldsymbol{g}})$.

An MEKF based on the Rodrigues-Gibbs vector would use Eq. (24) as written, but insight is gained by expressing $\hat{\boldsymbol{g}}$ in terms of the Euler axis and angle, which gives

$$\begin{aligned} \Gamma_g(\hat{\boldsymbol{e}},\hat{\vartheta}) &= \cos^2(\hat{\vartheta}/2)I_3 - \cos(\hat{\vartheta}/2)\sin(\hat{\vartheta}/2)[\hat{\boldsymbol{e}}\times] \\ &= A(\hat{\boldsymbol{e}},\hat{\vartheta}/2)H_g(\hat{\boldsymbol{e}},\hat{\vartheta}) \end{aligned} \tag{31}$$

where $A(\hat{\boldsymbol{e}},\hat{\vartheta}/2)$ rotates vectors about the Euler axis $\hat{\boldsymbol{e}}$ of the update by an Euler angle $\hat{\vartheta}/2$, and $H_g(\hat{\boldsymbol{e}},\hat{\vartheta})$ is a symmetric matrix given by

$$H_g(\hat{\boldsymbol{e}},\hat{\vartheta}) = \hat{\boldsymbol{e}}\hat{\boldsymbol{e}}^T\cos^2(\hat{\vartheta}/2) + \left(I_3 - \hat{\boldsymbol{e}}\hat{\boldsymbol{e}}^T\right)\cos(\hat{\vartheta}/2) \tag{32}$$

The three eigenvalues of $H_g(\hat{\boldsymbol{e}},\hat{\vartheta})$ are $\cos(\hat{\vartheta}/2)$, $\cos(\hat{\vartheta}/2)$, and $\cos^2(\hat{\vartheta}/2)$. Thus, errors perpendicular to the update are decreased by a factor of $\cos(\hat{\vartheta}/2)$ and errors parallel to the update are decreased by a factor of $\cos^2(\hat{\vartheta}/2)$, which both go to zero as $\vartheta \to 180°$, so P^+ goes to zero in this singular limit. Stretching and rotating in the reverse order produces the same result because the matrices $A(\hat{\boldsymbol{e}},\hat{\vartheta}/2)$ and $H_g(\hat{\boldsymbol{e}},\hat{\vartheta})$ commute.

In terms of the Euler axis and angle of the attitude update, Eqs. (26) and (30) are

$$\left\|H_g(\hat{\boldsymbol{e}},\hat{\vartheta})P_g\hat{\boldsymbol{e}}\sin\hat{\vartheta}\right\| \ll 2 \tag{33a}$$

$$\hat{\boldsymbol{e}}^T P_g\hat{\boldsymbol{e}}\sin^2\hat{\vartheta} \ll 4/3 \tag{33b}$$

These conditions do not appear to be difficult to satisfy.

B. Vector Part of the Quaternion

One might argue that the parameterization should be chosen so that $\|\boldsymbol{\delta}\|$ is proportional to the actual magnitude of the attitude error. One possibility is to say that the attitude error magnitude is the Frobenius norm of the difference between $\hat{A}$ and $A(\boldsymbol{\delta})\hat{A}$:

$$\begin{aligned} \|\hat{A} - A(\boldsymbol{\delta})\hat{A}\|_F^2 &= \text{trace}\left([\hat{A} - A(\boldsymbol{\delta})\hat{A}][\hat{A} - A(\boldsymbol{\delta})\hat{A}]^T \right) \\ &= 2\,\text{trace}\,[I_3 - A(\boldsymbol{\delta})] \end{aligned} \tag{34}$$

where $\|\cdot\|_F$ denotes the Frobenius norm. Using the quaternion parameterization of $A(\boldsymbol{\delta})$ gives

$$\begin{aligned} \|\hat{A} - A(\boldsymbol{\delta})\hat{A}\|_F &= \sqrt{2\left[3 - 3\left(q_4^2 - \|\boldsymbol{q}_{1:3}\|^2\right) - 2\|\boldsymbol{q}_{1:3}\|^2\right]} \\ &= \sqrt{8}\,\|\boldsymbol{q}_{1:3}\| \end{aligned} \tag{35}$$

This would indicate that $\boldsymbol{\delta} = \boldsymbol{q}_{1:3} = \boldsymbol{e}\sin(\vartheta/2)$, where $\boldsymbol{e}$ and ϑ are the Euler axis and angle of the attitude error, is a good choice for the attitude error parameterization, as was done in Section XI of [5]. In this parameterization $\boldsymbol{q}_{1:3}$ must be restricted to the 3D unit ball.

The attitude quaternion product rule in Eq. (5) gives Eq. (22) as the product

$$\begin{aligned} \boldsymbol{q}^+ &= \begin{bmatrix} \boldsymbol{q}_{1:3}^+ \\ \sqrt{1 - \|\boldsymbol{q}_{1:3}^+\|^2} \end{bmatrix} \\ &= \boldsymbol{q} \otimes \hat{\boldsymbol{q}}^{-1} \\ &= \begin{bmatrix} \boldsymbol{q}_{1:3} \\ \sqrt{1 - \|\boldsymbol{q}_{1:3}\|^2} \end{bmatrix} \otimes \begin{bmatrix} -\hat{\boldsymbol{q}}_{1:3} \\ \sqrt{1 - \|\hat{\boldsymbol{q}}_{1:3}\|^2} \end{bmatrix} \end{aligned} \tag{36}$$

With $\boldsymbol{q}_{1:3} = \hat{\boldsymbol{q}}_{1:3} + \Delta\boldsymbol{q}_{1:3}$, the vector part of this equation is

$$\boldsymbol{q}_{1:3}^+ = \sqrt{1 - \|\hat{\boldsymbol{q}}_{1:3}\|^2}\,(\hat{\boldsymbol{q}}_{1:3} + \Delta\boldsymbol{q}_{1:3}) - \sqrt{1 - \|\hat{\boldsymbol{q}}_{1:3} + \Delta\boldsymbol{q}_{1:3}\|^2}\,\hat{\boldsymbol{q}}_{1:3} + \Delta\boldsymbol{q}_{1:3} \times \hat{\boldsymbol{q}}_{1:3} \tag{37}$$

To prepare for computing expectations, the second square root in powers of $\boldsymbol{\Delta q}_{1:3}$ is expanded. This gives, to third order

$$\begin{aligned}\boldsymbol{q}_{1:3}^{+} = \Gamma_q\left(\hat{\boldsymbol{q}}_{1:3}\right)\boldsymbol{\Delta q}_{1:3} + \Bigg[& \frac{\left\|\boldsymbol{\Delta q}_{1:3}\right\|^2}{2\sqrt{1-\left\|\hat{\boldsymbol{q}}_{1:3}\right\|^2}} + \frac{\left(\hat{\boldsymbol{q}}_{1:3}\cdot\boldsymbol{\Delta q}_{1:3}\right)^2}{2\left(1-\left\|\hat{\boldsymbol{q}}_{1:3}\right\|^2\right)^{3/2}} \\ & + \frac{\left(\hat{\boldsymbol{q}}_{1:3}\cdot\boldsymbol{\Delta q}_{1:3}\right)\left\|\boldsymbol{\Delta q}_{1:3}\right\|^2}{2\left(1-\left\|\hat{\boldsymbol{q}}_{1:3}\right\|^2\right)^{3/2}} + \frac{\left(\hat{\boldsymbol{q}}_{1:3}\cdot\boldsymbol{\Delta q}_{1:3}\right)^3}{2\left(1-\left\|\hat{\boldsymbol{q}}_{1:3}\right\|^2\right)^{5/2}}\Bigg]\hat{\boldsymbol{q}}_{1:3}\end{aligned} \tag{38}$$

with

$$\begin{aligned}\Gamma_q\left(\hat{\boldsymbol{q}}_{1:3}\right) &= \frac{\left(1-\left\|\hat{\boldsymbol{q}}_{1:3}\right\|^2\right)I_3 + \hat{\boldsymbol{q}}_{1:3}\hat{\boldsymbol{q}}_{1:3}^T}{\sqrt{1-\left\|\hat{\boldsymbol{q}}_{1:3}\right\|^2}} - \left[\hat{\boldsymbol{q}}_{1:3}\times\right] \\ &= \frac{I_3 + \left[\hat{\boldsymbol{q}}_{1:3}\times\right]^2}{\sqrt{1-\left\|\hat{\boldsymbol{q}}_{1:3}\right\|^2}} - \left[\hat{\boldsymbol{q}}_{1:3}\times\right]\end{aligned} \tag{39}$$

Because the expectation of $\boldsymbol{\Delta q}_{1:3}$ is zero by definition, the expectation of Eq. (38) to lowest non-vanishing order is

$$\hat{\boldsymbol{q}}_{1:3}^{+} = \left[\frac{\operatorname{trace} P_q}{2\sqrt{1-\left\|\hat{\boldsymbol{q}}_{1:3}\right\|^2}} + \frac{\hat{\boldsymbol{q}}_{1:3}^T P_q \hat{\boldsymbol{q}}_{1:3}}{2\left(1-\left\|\hat{\boldsymbol{q}}_{1:3}\right\|^2\right)^{3/2}}\right]\hat{\boldsymbol{q}}_{1:3} \tag{40}$$

The reset sets $\hat{\boldsymbol{q}}_{1:3}^{+}$to zero, as stated below Eq. (20), and the two quantities inside the brackets are both positive, so consistency requires

$$\left(1-\left\|\hat{\boldsymbol{q}}_{1:3}\right\|^2\right)^{-1/2}\left(\operatorname{trace} P_q\right)\left\|\hat{\boldsymbol{q}}_{1:3}\right\| = \left(\operatorname{trace} P_q\right)\tan(\hat{\vartheta}/2) \ll 2 \tag{41a}$$

$$\left(1-\left\|\hat{\boldsymbol{q}}_{1:3}\right\|^2\right)^{-3/2}\hat{\boldsymbol{q}}_{1:3}^T P_q \hat{\boldsymbol{q}}_{1:3}\left\|\hat{\boldsymbol{q}}_{1:3}\right\| = \left(\hat{\boldsymbol{e}}^T P_q \hat{\boldsymbol{e}}\right)\tan^3(\hat{\vartheta}/2) \ll 2 \tag{41b}$$

It is difficult to satisfy these conditions if $\hat{\vartheta} \approx \pi$, the case for very large attitude updates.

If the expectation of odd-order terms in $\boldsymbol{\Delta q}_{1:3}$ is zero, then the post-reset error-covariance is

$$\begin{aligned}
P_q^+ &= E\left\{\boldsymbol{q}_{1:3}^+\left(\boldsymbol{q}_{1:3}^+\right)^T\right\} - \hat{\boldsymbol{q}}_{1:3}^+\left(\hat{\boldsymbol{q}}_{1:3}^+\right)^T = \Gamma_q\left(\hat{\boldsymbol{q}}_{1:3}\right) P_q \Gamma_q^T\left(\hat{\boldsymbol{q}}_{1:3}\right) - \hat{\boldsymbol{q}}_{1:3}^+\left(\hat{\boldsymbol{q}}_{1:3}^+\right)^T \\
&+ E\left\{\frac{\|\boldsymbol{\Delta q}_{1:3}\|^4}{4\left(1-\|\hat{\boldsymbol{q}}_{1:3}\|^2\right)} + \frac{\|\boldsymbol{\Delta q}_{1:3}\|^2\left(\hat{\boldsymbol{q}}_{1:3}\cdot\boldsymbol{\Delta q}_{1:3}\right)^2}{2\left(1-\|\hat{\boldsymbol{q}}_{1:3}\|^2\right)^2} + \frac{\left(\hat{\boldsymbol{q}}_{1:3}\cdot\boldsymbol{\Delta q}_{1:3}\right)^4}{4\left(1-\|\hat{\boldsymbol{q}}_{1:3}\|^2\right)^3}\right\}\hat{\boldsymbol{q}}_{1:3}\hat{\boldsymbol{q}}_{1:3}^T \\
&+ \hat{\boldsymbol{q}}_{1:3} E\left\{\left[\frac{\left(\hat{\boldsymbol{q}}_{1:3}\cdot\boldsymbol{\Delta q}_{1:3}\right)\|\boldsymbol{\Delta q}_{1:3}\|^2}{2\left(1-\|\hat{\boldsymbol{q}}_{1:3}\|^2\right)^{3/2}} + \frac{\left(\hat{\boldsymbol{q}}_{1:3}\cdot\boldsymbol{\Delta q}_{1:3}\right)^3}{2\left(1-\|\hat{\boldsymbol{q}}_{1:3}\|^2\right)^{5/2}}\right]\left(\boldsymbol{\Delta q}_{1:3}\right)^T\right\}\Gamma_q^T\left(\hat{\boldsymbol{q}}_{1:3}\right) \\
&+ \Gamma_q\left(\hat{\boldsymbol{q}}_{1:3}\right) E\left\{\left(\boldsymbol{\Delta q}_{1:3}\right)\left[\frac{\left(\hat{\boldsymbol{q}}_{1:3}\cdot\boldsymbol{\Delta q}_{1:3}\right)\|\boldsymbol{\Delta q}_{1:3}\|^2}{2\left(1-\|\hat{\boldsymbol{q}}_{1:3}\|^2\right)^{3/2}} + \frac{\left(\hat{\boldsymbol{q}}_{1:3}\cdot\boldsymbol{\Delta q}_{1:3}\right)^3}{2\left(1-\|\hat{\boldsymbol{q}}_{1:3}\|^2\right)^{5/2}}\right]\right\}\hat{\boldsymbol{q}}_{1:3}^T
\end{aligned} \tag{42}$$

to fourth order. Applying Isserlis' Theorem gives, after some cancellations, gives

$$\begin{aligned}
P_q^+ &= \Gamma_q\left(\hat{\boldsymbol{q}}_{1:3}\right) P_q \Gamma_q^T\left(\hat{\boldsymbol{q}}_{1:3}\right) \\
&+ \left[\frac{\left\|P_q\right\|_F^2}{2\left(1-\|\hat{\boldsymbol{q}}_{1:3}\|^2\right)} + \frac{\left\|P_q\hat{\boldsymbol{q}}_{1:3}\right\|^2}{\left(1-\|\hat{\boldsymbol{q}}_{1:3}\|^2\right)^2} + \frac{\left(\hat{\boldsymbol{q}}_{1:3}^T P_q \hat{\boldsymbol{q}}_{1:3}\right)^2}{2\left(1-\|\hat{\boldsymbol{q}}_{1:3}\|^2\right)^3}\right]\hat{\boldsymbol{q}}_{1:3}\hat{\boldsymbol{q}}_{1:3}^T \\
&+ \hat{\boldsymbol{q}}_{1:3}\hat{\boldsymbol{q}}_{1:3}^T\left[\frac{I_3\,\mathrm{trace}\,P_q + 2P_q}{2\left(1-\|\hat{\boldsymbol{q}}_{1:3}\|^2\right)^{3/2}} + \frac{3\hat{\boldsymbol{q}}_{1:3}^T P_q \hat{\boldsymbol{q}}_{1:3}}{2\left(1-\|\hat{\boldsymbol{q}}_{1:3}\|^2\right)^{5/2}}\right] P_q \Gamma_q^T\left(\hat{\boldsymbol{q}}_{1:3}\right) \\
&+ \Gamma_q\left(\hat{\boldsymbol{q}}_{1:3}\right) P_q\left[\frac{I_3\,\mathrm{trace}\,P_q + 2P_q}{2\left(1-\|\hat{\boldsymbol{q}}_{1:3}\|^2\right)^{3/2}} + \frac{3\hat{\boldsymbol{q}}_{1:3}^T P_q \hat{\boldsymbol{q}}_{1:3}}{2\left(1-\|\hat{\boldsymbol{q}}_{1:3}\|^2\right)^{5/2}}\right]\hat{\boldsymbol{q}}_{1:3}\hat{\boldsymbol{q}}_{1:3}^T
\end{aligned} \tag{43}$$

The conditions for $P_p^+ = \Gamma_q(\hat{\boldsymbol{q}}_{1:3}) P_p \Gamma_q^T(\hat{\boldsymbol{q}}_{1:3})$ to give an accurate reset are clearly more intricate than those for the Rodrigues-Gibbs parameterization.

Expressing $\hat{\boldsymbol{q}}_{1:3}$ in terms of the Euler axis and angle gives

$$\begin{aligned}
\Gamma_q(\hat{\boldsymbol{e}},\hat{\vartheta}) &= \frac{I_3 + \sin^2(\hat{\vartheta}/2)[\hat{\boldsymbol{e}}\times]^2}{\cos(\hat{\vartheta}/2)} - \sin(\hat{\vartheta}/2)[\hat{\boldsymbol{e}}\times] \\
&= A(\hat{\boldsymbol{e}},\hat{\vartheta}/2) H_q(\hat{\boldsymbol{e}},\hat{\vartheta})
\end{aligned} \tag{44}$$

where $H_q(\hat{\boldsymbol{e}},\hat{\vartheta})$ is a symmetric matrix given by

$$H_q(\hat{\boldsymbol{e}},\hat{\vartheta}) = \frac{\hat{\boldsymbol{e}}\hat{\boldsymbol{e}}^T}{\cos(\hat{\vartheta}/2)} + \left(I_3 - \hat{\boldsymbol{e}}\hat{\boldsymbol{e}}^T\right) \tag{45}$$

The three eigenvalues of $H_q(\hat{\boldsymbol{e}},\hat{\vartheta})$ are 1, 1, and $1/\cos(\hat{\vartheta}/2)$. The matrix $H_q(\hat{\boldsymbol{e}},\hat{\vartheta})$ leaves the magnitude of errors

perpendicular to the update unchanged and increases the magnitude of errors parallel to the update by a factor of $1/\cos(\hat{\vartheta}/2)$, which becomes infinite as $\hat{\vartheta} \to 180°$.

The following heuristic argument "explains" the ratios of the scale factors of H_g and H_q. The Rodrigues-Gibbs reset and the quaternion reset move the errors from distributions centered on $\hat{\boldsymbol{e}} \tan(\hat{\vartheta}/2)$ or $\hat{\boldsymbol{e}} \sin(\hat{\vartheta}/2)$, respectively, to distributions centered on the origin, where small-angle trigonometric approximations can be used. Thus, it would be expected that the ratio of the H_g and H_q magnifications of errors perpendicular to the update axis to be

$$\frac{(\hat{\vartheta}/2)}{\tan(\hat{\vartheta}/2)} \cdot \frac{(\hat{\vartheta}/2)}{\sin(\hat{\vartheta}/2)} = \frac{\sin(\hat{\vartheta}/2)}{\tan(\hat{\vartheta}/2)} = \cos(\hat{\vartheta}/2) \tag{46}$$

as it is. Similarly, it would be expected that the ratio of the magnifications of errors parallel to the update axis to be

$$\frac{d \sin(\hat{\vartheta}/2)}{d\hat{\vartheta}} \cdot \frac{d \tan(\hat{\vartheta}/2)}{d\hat{\vartheta}} = \cos^3(\hat{\vartheta}/2) \tag{47}$$

also as it is.

C. Modified Rodrigues Parameter Parameterization

The product rule in Eq. (18) for the MRP attitude-error parameterization $\boldsymbol{\delta} = \boldsymbol{p} = \boldsymbol{e} \tan(\vartheta/4)$ expresses Eq. (22) as

$$\begin{aligned}
\boldsymbol{p}^+ &= \frac{\left(1 - \|\hat{\boldsymbol{p}}\|^2\right) \boldsymbol{p} - \left(1 - \|\boldsymbol{p}\|^2\right) \hat{\boldsymbol{p}} + 2\boldsymbol{p} \times \hat{\boldsymbol{p}}}{1 + \|\boldsymbol{p}\|^2 \|\hat{\boldsymbol{p}}\|^2 + 2\boldsymbol{p} \cdot \hat{\boldsymbol{p}}} \\
&= \frac{\left\{\left(1 - \|\hat{\boldsymbol{p}}\|^2\right) I_3 + 2\hat{\boldsymbol{p}}\hat{\boldsymbol{p}}^T - 2[\hat{\boldsymbol{p}}\times]\right\} \boldsymbol{\Delta p} + \|\boldsymbol{\Delta p}\|^2 \hat{\boldsymbol{p}}}{\left(1 + \|\hat{\boldsymbol{p}}\|^2\right)\left(1 + \|\hat{\boldsymbol{p}}\|^2 + 2\hat{\boldsymbol{p}} \cdot \boldsymbol{\Delta p}\right) + \|\boldsymbol{\Delta p}\|^2 \|\hat{\boldsymbol{p}}\|^2} \\
&= \left[\Gamma_p(\hat{\boldsymbol{p}}) \boldsymbol{\Delta p} + \frac{\|\boldsymbol{\Delta p}\|^2 \hat{\boldsymbol{p}}}{\left(1 + \|\hat{\boldsymbol{p}}\|^2\right)^2}\right]\left[1 - \frac{2\hat{\boldsymbol{p}} \cdot \boldsymbol{\Delta p}}{1 + \|\hat{\boldsymbol{p}}\|^2} - \left(\frac{\|\boldsymbol{\Delta p}\| \|\hat{\boldsymbol{p}}\|}{1 + \|\hat{\boldsymbol{p}}\|^2}\right)^2 + \left(\frac{2\hat{\boldsymbol{p}} \cdot \boldsymbol{\Delta p}}{1 + \|\hat{\boldsymbol{p}}\|^2}\right)^2 + \ldots\right]
\end{aligned} \tag{48}$$

with

$$\Gamma_p(\hat{\boldsymbol{p}}) \equiv \frac{\left(1 - \|\hat{\boldsymbol{p}}\|^2\right) I_3 + 2\hat{\boldsymbol{p}}\hat{\boldsymbol{p}}^T - 2[\hat{\boldsymbol{p}}\times]}{\left(1 + \|\hat{\boldsymbol{p}}\|^2\right)^2} \tag{49}$$

The expectation of $\boldsymbol{\Delta p}$ vanishes by definition. Retaining only the lowest-order nonzero terms, the expectation of Eq. (48) is

$$\hat{\boldsymbol{p}}^+ = \left[\frac{I_3 \operatorname{trace} P_p}{\left(1 + \|\hat{\boldsymbol{p}}\|^2\right)^2} - 2\frac{\Gamma_p(\hat{\boldsymbol{p}}) P_p}{1 + \|\hat{\boldsymbol{p}}\|^2}\right] \hat{\boldsymbol{p}} \tag{50}$$

The reset sets $\hat{\boldsymbol{p}}^+$ to zero, as stated below Eq. (20), so consistency requires the magnitude of the right side of this equation to be much less than unity.

Assuming that expectations of odd powers of $\boldsymbol{\Delta p}$ vanish, the post-update error-covariance is

$$\begin{aligned} P_p^+ &= E\left\{\boldsymbol{p}^+\left(\boldsymbol{p}^+\right)^T\right\} - \hat{\boldsymbol{p}}^+\left(\hat{\boldsymbol{p}}^+\right)^T \\ &= \Gamma_p(\hat{\boldsymbol{p}})P_p\Gamma_p^T(\hat{\boldsymbol{p}}) + \left(1+\|\hat{\boldsymbol{p}}\|^2\right)^{-2}\Gamma_p(\hat{\boldsymbol{p}})E\left\{\left[12(\hat{\boldsymbol{p}}\cdot\boldsymbol{\Delta p})^2 - 2\|\boldsymbol{\Delta p}\|^2\|\hat{\boldsymbol{p}}\|^2\right]\boldsymbol{\Delta p}\boldsymbol{\Delta p}^T\right\}\Gamma_p^T(\hat{\boldsymbol{p}}) \\ &- 2\left(1+\|\hat{\boldsymbol{p}}\|^2\right)^{-3}\left[\Gamma_p(\hat{\boldsymbol{p}})E\left\{\boldsymbol{\Delta p}(\hat{\boldsymbol{p}}\cdot\boldsymbol{\Delta p})\|\boldsymbol{\Delta p}\|^2\right\}\hat{\boldsymbol{p}}^T + \hat{\boldsymbol{p}}E\left\{\|\boldsymbol{\Delta p}\|^2(\hat{\boldsymbol{p}}\cdot\boldsymbol{\Delta p})\boldsymbol{\Delta p}^T\right\}\Gamma_p^T(\hat{\boldsymbol{p}})\right] \\ &+ \left(1+\|\hat{\boldsymbol{p}}\|^2\right)^{-4}E\left\{\|\boldsymbol{\Delta p}\|^4\right\}\hat{\boldsymbol{p}}\hat{\boldsymbol{p}}^T - \hat{\boldsymbol{p}}^+\left(\hat{\boldsymbol{p}}^+\right)^T \end{aligned} \tag{51}$$

to fourth order. Applying Isserlis' Theorem gives, after some cancellations, gives

$$\begin{aligned} P_p^+ &= \Gamma_p(\hat{\boldsymbol{p}})P_p\Gamma_p^T(\hat{\boldsymbol{p}})\left[1+2\left(1+\|\hat{\boldsymbol{p}}\|^2\right)^{-2}\left(6\hat{\boldsymbol{p}}^TP_p\hat{\boldsymbol{p}} - \|\hat{\boldsymbol{p}}\|^2\,\mathrm{trace}\,P_p\right)\right] \\ &+ 4\left(1+\|\hat{\boldsymbol{p}}\|^2\right)^{-2}\Gamma_p(\hat{\boldsymbol{p}})P_p\left(5\hat{\boldsymbol{p}}\hat{\boldsymbol{p}}^T - \|\hat{\boldsymbol{p}}\|^2I_3\right)P_p\Gamma_p^T(\hat{\boldsymbol{p}}) \\ &- 4\left(1+\|\hat{\boldsymbol{p}}\|^2\right)^{-3}\left[\Gamma_p(\hat{\boldsymbol{p}})P_p^2\hat{\boldsymbol{p}}\hat{\boldsymbol{p}}^T + \hat{\boldsymbol{p}}\hat{\boldsymbol{p}}^TP_p^2\Gamma_p^T(\hat{\boldsymbol{p}})\right] + 2\left(1+\|\hat{\boldsymbol{p}}\|^2\right)^{-4}\left\|P_p\right\|_F^2\hat{\boldsymbol{p}}\hat{\boldsymbol{p}}^T \end{aligned} \tag{52}$$

The conditions for $P_p^+ = \Gamma_p(\hat{\boldsymbol{p}})P_p\Gamma_p^T(\hat{\boldsymbol{p}})$ to give an accurate reset are clearly more intricate than those for the Rodrigues-Gibbs parameterization.

Expressing $\hat{\boldsymbol{p}}$ in terms of the Euler axis and angle gives

$$\Gamma_p(\hat{\boldsymbol{e}},\hat{\vartheta}) = \cos^2(\hat{\vartheta}/4)A(\hat{\boldsymbol{e}},\hat{\vartheta}/2) \tag{53}$$

The matrix $\Gamma_p(\hat{\boldsymbol{e}},\hat{\vartheta})$ rotates all errors by an angle $\hat{\vartheta}/2$ about $\hat{\boldsymbol{e}}$ and decreases their magnitude by a factor of $\cos^2(\hat{\vartheta}/4)$, which goes to $1/2$ as $\vartheta \to 180°$.

D. Rotation Vector Parameterization

Finally, consider the rotation vector error parameterization $\boldsymbol{\delta} = \boldsymbol{\vartheta} = \vartheta\boldsymbol{e}$. From Eq. (37)

$$\begin{aligned} \sin\left(\vartheta^+/2\right)\boldsymbol{e}^+ &= \cos(\hat{\vartheta}/2)\sin(\vartheta/2)\boldsymbol{e} - \cos(\vartheta/2)\sin(\hat{\vartheta}/2)\hat{\boldsymbol{e}} + \sin(\vartheta/2)\sin(\hat{\vartheta}/2)\boldsymbol{e}\times\hat{\boldsymbol{e}} \\ &\equiv \boldsymbol{w}/2 \end{aligned} \tag{54}$$

It is clear from this equation that $\sin(\vartheta^+/2) = \|\boldsymbol{w}\|/2$ and $\boldsymbol{e}^+ = \boldsymbol{w}/\|\boldsymbol{w}\|$, so

$$\begin{aligned} \boldsymbol{\vartheta}^+ &= \vartheta^+\boldsymbol{e}^+ \\ &= (2/\|\boldsymbol{w}\|)\sin^{-1}(\|\boldsymbol{w}\|/2)\boldsymbol{w} \\ &= \left(1+\|\boldsymbol{w}\|^2/24\right)\boldsymbol{w} \end{aligned} \tag{55}$$

to third order in $\|\boldsymbol{w}\|$. It is also clear that $\boldsymbol{e} = (\hat{\boldsymbol{\vartheta}} + \Delta\boldsymbol{\vartheta})/\vartheta = (\hat{\vartheta}\hat{\boldsymbol{e}} + \Delta\boldsymbol{\vartheta})/\vartheta$, so

$$\begin{aligned}\boldsymbol{w} &= 2\vartheta^{-1}[\cos(\hat{\vartheta}/2)\sin(\vartheta/2)(\hat{\boldsymbol{\vartheta}} + \Delta\boldsymbol{\vartheta}) - \cos(\vartheta/2)\sin(\hat{\vartheta}/2)(\vartheta\hat{\boldsymbol{e}}) + \sin(\vartheta/2)\sin(\hat{\vartheta}/2)\Delta\boldsymbol{\vartheta}\times\hat{\boldsymbol{e}}] \\ &= 2\vartheta^{-1}[\sin((\vartheta-\hat{\vartheta})/2)\hat{\boldsymbol{\vartheta}} + \cos(\hat{\vartheta}/2)\sin(\vartheta/2)\Delta\boldsymbol{\vartheta} - \cos(\vartheta/2)\sin(\hat{\vartheta}/2)(\vartheta-\hat{\vartheta})\hat{\boldsymbol{e}} \\ &\quad + \sin(\vartheta/2)\sin(\hat{\vartheta}/2)\Delta\boldsymbol{\vartheta}\times\hat{\boldsymbol{e}}]\end{aligned} \tag{56}$$

Also, to third order in $\|\Delta\boldsymbol{\vartheta}\|$, the following expression is given:

$$\begin{aligned}\vartheta &= \pm\sqrt{\|\hat{\boldsymbol{\vartheta}} + \Delta\boldsymbol{\vartheta}\|^2} \\ &= \hat{\vartheta}\sqrt{1 + 2(\hat{\boldsymbol{e}}\cdot\Delta\boldsymbol{\vartheta})/\hat{\vartheta} + (\|\Delta\boldsymbol{\vartheta}\|/\hat{\vartheta})^2} \\ &= \hat{\vartheta} + \hat{\boldsymbol{e}}\cdot\Delta\boldsymbol{\vartheta} + \frac{\|\hat{\boldsymbol{e}}\times\Delta\boldsymbol{\vartheta}\|^2}{2\hat{\vartheta}} - \frac{(\hat{\boldsymbol{e}}\cdot\Delta\boldsymbol{\vartheta})\|\hat{\boldsymbol{e}}\times\Delta\boldsymbol{\vartheta}\|^2}{2\hat{\vartheta}^2} \\ &\equiv \hat{\vartheta} + \vartheta_1 + \vartheta_2 + \vartheta_3\end{aligned} \tag{57}$$

where a subscript ℓ will be used to identify a term of order ℓ in $\|\Delta\boldsymbol{\vartheta}\|$. The sign of the square root is chosen so that $\vartheta = \hat{\vartheta}$ for $\Delta\boldsymbol{\vartheta} = \boldsymbol{0}$. Substituting this into Eq. (56) gives

$$\begin{aligned}\boldsymbol{w} &= 2\vartheta^{-1}\Big\{\sin\left[\left(\vartheta_1+\vartheta_2+\vartheta_3\right)/2\right]\hat{\boldsymbol{\vartheta}} + \cos(\hat{\vartheta}/2)\sin\left[\left(\hat{\vartheta}+\vartheta_1+\vartheta_2\right)/2\right]\Delta\boldsymbol{\vartheta} \\ &\quad - \cos\left[\left(\hat{\vartheta}+\vartheta_1+\vartheta_2\right)/2\right]\sin(\hat{\vartheta}/2)\left(\vartheta_1+\vartheta_2+\vartheta_3\right)\hat{\boldsymbol{e}} \\ &\quad + \sin\left[\left(\hat{\vartheta}+\vartheta_1+\vartheta_2\right)/2\right]\sin(\hat{\vartheta}/2)\Delta\boldsymbol{\vartheta}\times\hat{\boldsymbol{e}}\Big\} \\ &= \vartheta^{-1}\left[\boldsymbol{v}_1+\boldsymbol{v}_2+\boldsymbol{v}_3\right] \\ &\equiv \boldsymbol{w}_1+\boldsymbol{w}_2+\boldsymbol{w}_3\end{aligned} \tag{58}$$

Expanding and collecting terms gives

$$\boldsymbol{v}_1 = \left\{\sin\hat{\vartheta}I_3 + (\hat{\vartheta}-\sin\hat{\vartheta})\hat{\boldsymbol{e}}\hat{\boldsymbol{e}}^T - (1-\cos\hat{\vartheta})[\hat{\boldsymbol{e}}\times]\right\}\Delta\boldsymbol{\vartheta} \tag{59a}$$

$$\boldsymbol{v}_2 = (1/2)\left\{\|\hat{\boldsymbol{e}}\times\Delta\boldsymbol{\vartheta}\|^2[(\hat{\vartheta}-\sin\hat{\vartheta})/\hat{\vartheta}]I_3 + \left[I_3 + A(\hat{\boldsymbol{e}},\hat{\vartheta})\right]\Delta\boldsymbol{\vartheta}\Delta\boldsymbol{\vartheta}^T\right\}\hat{\boldsymbol{e}} \tag{59b}$$

$$\begin{aligned}\boldsymbol{v}_3 = \frac{\|\hat{\boldsymbol{e}}\times\Delta\boldsymbol{\vartheta}\|^2}{4\hat{\vartheta}}&\left\{I_3 + A(\hat{\boldsymbol{e}},\hat{\vartheta}) + [1-\cos\hat{\vartheta} - 2(\hat{\vartheta}-\sin\hat{\vartheta})/\hat{\vartheta}]\hat{\boldsymbol{e}}\hat{\boldsymbol{e}}^T\right\}\Delta\boldsymbol{\vartheta} \\ &+ \left[(\hat{\boldsymbol{e}}\cdot\Delta\boldsymbol{\vartheta})^2/8\right]\left\{\sin\hat{\vartheta}[\hat{\boldsymbol{e}}\times]^2 + (1-\cos\hat{\vartheta})[\hat{\boldsymbol{e}}\times] - (\hat{\vartheta}/3)\hat{\boldsymbol{e}}\hat{\boldsymbol{e}}^T\right\}\Delta\boldsymbol{\vartheta}\end{aligned} \tag{59c}$$

It is found from Eq. (57) that

$$\vartheta^{-1} = \hat{\vartheta}^{-1}\left[1 - \frac{\hat{\boldsymbol{e}}\cdot\Delta\boldsymbol{\vartheta}}{\hat{\vartheta}} + \left(\frac{\hat{\boldsymbol{e}}\cdot\Delta\boldsymbol{\vartheta}}{\hat{\vartheta}}\right)^2 - \frac{\|\hat{\boldsymbol{e}}\times\Delta\boldsymbol{\vartheta}\|^2}{2\hat{\vartheta}^2}\right] \tag{60}$$

to second order in $\|\boldsymbol{\Delta\vartheta}\|$. This and Eq. (58) give

$$\boldsymbol{w}_1 = \hat{\vartheta}^{-1}\boldsymbol{v}_1 = \Gamma_\vartheta(\hat{\boldsymbol{\vartheta}})\boldsymbol{\Delta\vartheta} \tag{61}$$

with

$$\Gamma_\vartheta(\hat{\boldsymbol{\vartheta}}) = I_3 - \frac{1-\cos\hat{\vartheta}}{\hat{\vartheta}}[\hat{\boldsymbol{e}}\times] + \frac{\hat{\vartheta}-\sin\hat{\vartheta}}{\hat{\vartheta}}[\hat{\boldsymbol{e}}\times]^2 = A(\hat{\boldsymbol{e}},\hat{\vartheta}/2)H_\vartheta(\hat{\boldsymbol{\vartheta}}) \tag{62a}$$

$$H_\vartheta(\hat{\boldsymbol{\vartheta}}) = \hat{\boldsymbol{e}}\hat{\boldsymbol{e}}^T + \left(I_3 - \hat{\boldsymbol{e}}\hat{\boldsymbol{e}}^T\right)(2/\hat{\vartheta})\sin(\hat{\vartheta}/2) \tag{62b}$$

The three eigenvalues of $H_\vartheta(\hat{\boldsymbol{\vartheta}})$ are $(2/\hat{\vartheta})\sin(\hat{\vartheta}/2)$, $(2/\hat{\vartheta})\sin(\hat{\vartheta}/2)$, and 1.

It is also found that

$$\begin{aligned}\boldsymbol{w}_2 &= \hat{\vartheta}^{-1}\left[\boldsymbol{v}_2 - (\hat{\boldsymbol{e}}\cdot\boldsymbol{\Delta\vartheta})\Gamma_\vartheta(\hat{\boldsymbol{\vartheta}})\boldsymbol{\Delta\vartheta}\right]\\ &= (2\hat{\vartheta})^{-1}\left\{\|\hat{\boldsymbol{e}}\times\boldsymbol{\Delta\vartheta}\|^2\left[(\hat{\vartheta}-\sin\hat{\vartheta})/\hat{\vartheta}\right]I_3 + \left[I_3 + A(\hat{\boldsymbol{e}},\hat{\vartheta}) - 2\Gamma_\vartheta(\hat{\boldsymbol{\vartheta}})\right]\boldsymbol{\Delta\vartheta}\boldsymbol{\Delta\vartheta}^T\right\}\hat{\boldsymbol{e}}\end{aligned} \tag{63}$$

and

$$\boldsymbol{w}_3 = \hat{\vartheta}^{-1}\left[\boldsymbol{v}_3 - (\hat{\boldsymbol{e}}\cdot\boldsymbol{\Delta\vartheta})\boldsymbol{w}_2\right] - \left(2\hat{\vartheta}^2\right)^{-1}\|\hat{\boldsymbol{e}}\times\boldsymbol{\Delta\vartheta}\|^2\Gamma_\vartheta(\hat{\boldsymbol{\vartheta}})\boldsymbol{\Delta\vartheta} \tag{64}$$

Because $\boldsymbol{\Delta\vartheta}$ has zero expectation, Eqs. (58), (61), and (63) give, to second order,

$$\begin{aligned}\hat{\boldsymbol{\vartheta}}^+ &= (2\hat{\vartheta})^{-1}\left\{\left(\text{trace}\,P_\vartheta - \hat{\boldsymbol{e}}^T P_\vartheta\hat{\boldsymbol{e}}\right)\left[(\hat{\vartheta}-\sin\hat{\vartheta})/\hat{\vartheta}\right]I_3 + \left[I_3 + A(\hat{\boldsymbol{e}},\hat{\vartheta}) - 2\Gamma_\vartheta(\hat{\boldsymbol{\vartheta}})\right]P_\vartheta\right\}\hat{\boldsymbol{e}}\\ &\approx (1/12)\left\{\left(\text{trace}\,P_\vartheta - \hat{\boldsymbol{e}}^T P_\vartheta\hat{\boldsymbol{e}}\right)I_3 + [\hat{\boldsymbol{e}}\times]^2 P_\vartheta\right\}\hat{\boldsymbol{\vartheta}} \quad \text{for } |\hat{\vartheta}| \ll 1\end{aligned} \tag{65}$$

The reset sets $\hat{\boldsymbol{\vartheta}}^+$to zero, so consistency requires $\left\|\hat{\boldsymbol{\vartheta}}^+\right\| \ll 1$.

Assuming that the expectations of odd powers of $\boldsymbol{\Delta\vartheta}$ vanish, the post-reset error-covariance to lowest non-vanishing order is

$$\begin{aligned}P_\vartheta^+ &= E\left\{\boldsymbol{\vartheta}^+\left(\boldsymbol{\vartheta}^+\right)^T\right\} - \hat{\boldsymbol{\vartheta}}^+\left(\hat{\boldsymbol{\vartheta}}^+\right)^T\\ &= E\left\{\left(\boldsymbol{w} + \|\boldsymbol{w}\|^2\boldsymbol{w}/24\right)\left(\boldsymbol{w} + \|\boldsymbol{w}\|^2\boldsymbol{w}/24\right)^T\right\} - \hat{\boldsymbol{\vartheta}}^+\left(\hat{\boldsymbol{\vartheta}}^+\right)^T\\ &= E\left\{\left[\Gamma_\vartheta(\hat{\boldsymbol{\vartheta}})\boldsymbol{\Delta\vartheta} + \boldsymbol{w}_2 + \overline{\boldsymbol{w}}_3\right]\left[\Gamma_\vartheta(\hat{\boldsymbol{\vartheta}})\boldsymbol{\Delta\vartheta} + \boldsymbol{w}_2 + \overline{\boldsymbol{w}}_3\right]^T\right\}\\ &= \Gamma_\vartheta(\hat{\boldsymbol{\vartheta}})P_\vartheta\Gamma_\vartheta^T(\hat{\boldsymbol{\vartheta}}) + \Gamma_\vartheta(\hat{\boldsymbol{\vartheta}})E\left\{\boldsymbol{\Delta\vartheta}\overline{\boldsymbol{w}}_3^T\right\} + E\left\{\overline{\boldsymbol{w}}_3\boldsymbol{\Delta\vartheta}^T\right\}\Gamma_\vartheta^T(\hat{\boldsymbol{\vartheta}}) + E\left\{\boldsymbol{w}_2\boldsymbol{w}_2^T\right\} - \hat{\boldsymbol{\vartheta}}^+\left(\hat{\boldsymbol{\vartheta}}^+\right)^T\end{aligned} \tag{66}$$

where

$$\begin{aligned}\overline{\boldsymbol{w}}_3 &= \boldsymbol{w}_3 + (1/24)\left\|\Gamma_\vartheta(\hat{\boldsymbol{\vartheta}})\boldsymbol{\Delta\vartheta}\right\|^2\Gamma_\vartheta(\hat{\boldsymbol{\vartheta}})\boldsymbol{\Delta\vartheta} = \boldsymbol{w}_3 + (1/24)\left[\boldsymbol{\Delta\vartheta}^T H_\vartheta^2(\hat{\boldsymbol{\vartheta}})\boldsymbol{\Delta\vartheta}\right]\Gamma_\vartheta(\hat{\boldsymbol{\vartheta}})\boldsymbol{\Delta\vartheta}\\ &= \boldsymbol{w}_3 + (1/24)\left[(\hat{\boldsymbol{e}}\cdot\boldsymbol{\Delta\vartheta})^2 + 2\hat{\vartheta}^{-2}(1-\cos\hat{\vartheta})\|\hat{\boldsymbol{e}}\times\boldsymbol{\Delta\vartheta}\|^2\right]\Gamma_\vartheta(\hat{\boldsymbol{\vartheta}})\boldsymbol{\Delta\vartheta}\end{aligned} \tag{67}$$

Combining this with Eqs. (59c), (63), and (64) gives

$$\begin{aligned}\overline{\boldsymbol{w}}_3 = \frac{\|\hat{\boldsymbol{e}} \times \boldsymbol{\Delta\vartheta}\|^2}{12\hat{\vartheta}^2}\left[3I_3 + 3A(\hat{\boldsymbol{e}},\hat{\vartheta}) - (5+\cos\hat{\vartheta})\Gamma_{\vartheta}(\hat{\boldsymbol{\vartheta}}) + 3\left(1-\cos\hat{\vartheta} - 4\frac{\hat{\vartheta}-\sin\hat{\vartheta}}{\hat{\vartheta}}\right)\hat{\boldsymbol{e}}\hat{\boldsymbol{e}}^T\right]\boldsymbol{\Delta\vartheta} \\ - \frac{(\hat{\boldsymbol{e}}\cdot\boldsymbol{\Delta\vartheta})^2}{12\hat{\vartheta}^2}\left[6I_3 + 6A(\hat{\boldsymbol{e}},\hat{\vartheta}) - \left(12-\hat{\vartheta}^2\right)\Gamma_{\vartheta}(\hat{\boldsymbol{\vartheta}}) - \hat{\vartheta}^2\hat{\boldsymbol{e}}\hat{\boldsymbol{e}}^T\right]\boldsymbol{\Delta\vartheta}\end{aligned} \tag{68}$$

This equation is intractable, but for $|\hat{\vartheta}| \ll 1$ the following are given:

$$\boldsymbol{w}_2 \approx (1/12)\left\{\|\hat{\boldsymbol{e}}\times\boldsymbol{\Delta\vartheta}\|^2 I_3 + [\hat{\boldsymbol{e}}\times]^2\boldsymbol{\Delta\vartheta}\boldsymbol{\Delta\vartheta}^T\right\}\hat{\boldsymbol{\vartheta}} \tag{69a}$$

$$\overline{\boldsymbol{w}}_3 \approx -(1/720)\left\{4\|\hat{\boldsymbol{\vartheta}}\times\boldsymbol{\Delta\vartheta}\|^2 I_3 + \|\boldsymbol{\Delta\vartheta}\|^2[\hat{\boldsymbol{\vartheta}}\times]^2\right\}\boldsymbol{\Delta\vartheta} \tag{69b}$$

Inserting these expressions into Eq. (66) gives, to second order in $\hat{\boldsymbol{\vartheta}}$,

$$\begin{aligned}P_{\vartheta}^+ \approx{}& \Gamma_{\vartheta}(\hat{\boldsymbol{\vartheta}})P_{\vartheta}\Gamma_{\vartheta}^T(\hat{\boldsymbol{\vartheta}}) - \hat{\boldsymbol{\vartheta}}^+\left(\hat{\boldsymbol{\vartheta}}^+\right)^T \\ &+ \left(\hat{\vartheta}^2/720\right)\left[5E\left\{\|\boldsymbol{\Delta\vartheta}\|^4\right\}\hat{\boldsymbol{e}}\hat{\boldsymbol{e}}^T + 13E\left\{(\hat{\boldsymbol{e}}\cdot\boldsymbol{\Delta\vartheta})^2\boldsymbol{\Delta\vartheta}\boldsymbol{\Delta\vartheta}^T\right\}\right. \\ &\left.-6E\left\{\|\boldsymbol{\Delta\vartheta}\|^2\boldsymbol{\Delta\vartheta}\boldsymbol{\Delta\vartheta}^T\right\} - 6E\left\{\|\boldsymbol{\Delta\vartheta}\|^2\boldsymbol{\Delta\vartheta}\boldsymbol{\Delta\vartheta}^T\right\}\hat{\boldsymbol{e}}\hat{\boldsymbol{e}}^T - 6\hat{\boldsymbol{e}}\hat{\boldsymbol{e}}^T E\left\{\|\boldsymbol{\Delta\vartheta}\|^2\boldsymbol{\Delta\vartheta}\boldsymbol{\Delta\vartheta}^T\right\}\right]\end{aligned} \tag{70}$$

after some algebraic manipulation. Using Isserlis' Theorem to find the expectations leads to the final second-order expression, given by

$$\begin{aligned}P_{\vartheta}^+ \approx{}& \Gamma_{\vartheta}(\hat{\boldsymbol{\vartheta}})P_{\vartheta}\Gamma_{\vartheta}^T(\hat{\boldsymbol{\vartheta}}) + \left(\hat{\vartheta}^2/720\right)\left\{10\,\|P_{\vartheta}\|_F^2\,\hat{\boldsymbol{e}}\hat{\boldsymbol{e}}^T + 13\left(\hat{\boldsymbol{e}}^T P_{\vartheta}\hat{\boldsymbol{e}}\right)P_{\vartheta} + 21\,(P_{\vartheta}\hat{\boldsymbol{e}})\,(P_{\vartheta}\hat{\boldsymbol{e}})^T\right. \\ &\left.- \operatorname{trace}P_{\vartheta}\left[6P_{\vartheta} + (P_{\vartheta}\hat{\boldsymbol{e}})\,\hat{\boldsymbol{e}}^T + \hat{\boldsymbol{e}}\,(P_{\vartheta}\hat{\boldsymbol{e}})^T\right] - 12\left[P_{\vartheta}^2 + \left(P_{\vartheta}^2\hat{\boldsymbol{e}}\right)\hat{\boldsymbol{e}}^T + \hat{\boldsymbol{e}}\left(P_{\vartheta}^2\hat{\boldsymbol{e}}\right)^T\right]\right\}\end{aligned} \tag{71}$$

The matrix Γ_{ϑ} rotates attitude errors by $\hat{\vartheta}/2$ about the attitude update axis. It leaves the magnitude of errors parallel to the update unchanged and decreases the magnitude of errors perpendicular to the update by a factor of $(2/\hat{\vartheta})\sin(\hat{\vartheta}/2)$, which goes to $2/\pi$ as $\hat{\vartheta} \to 180°$.

If $\boldsymbol{\Delta\vartheta}$ is parallel to $\hat{\boldsymbol{\vartheta}}$, then Eq. (22) in this paper and Eq. (2.117) in[12] say that $\boldsymbol{\vartheta}^+ = \boldsymbol{\vartheta} - \hat{\boldsymbol{\vartheta}} = \boldsymbol{\Delta\vartheta}$. All the parameterizations considered so far give the correct direction for $\boldsymbol{\delta}^+$ in this case, but only Γ_{ϑ} gives the correct magnitude of $\|\boldsymbol{\delta}^+\|$ to greater than first order in the update, and it gives the correct magnitude and direction to all orders.

V. Alternative Attitude Error-Covariance Reset

In the previous section, the attitude error-covariance reset matrices are derived by linearizing the nonlinear mapping $\boldsymbol{\Delta\delta} \to \boldsymbol{\delta}^+$ under the assumption that $\boldsymbol{\Delta\delta}$ is small. Based on the concept of projection onto the tangent space of the unit quaternion manifold, a slightly different attitude error-covariance reset matrix for the Rodrigues-Gibbs vector is given

by [13]

$$\Gamma'_g(\hat{\boldsymbol{g}}) \equiv \frac{I_3 - [\hat{\boldsymbol{g}}\times]}{\sqrt{1 + \|\hat{\boldsymbol{g}}\|^2}} \tag{72}$$

See [13] for the derivation. This matrix appears in an equivalent form of Eq. (23):

$$\begin{aligned} \frac{\boldsymbol{g}^+}{\sqrt{1 + \|\boldsymbol{g}^+\|^2}} =& \frac{I_3 - [\hat{\boldsymbol{g}}\times]}{\sqrt{1 + \|\hat{\boldsymbol{g}}\|^2}} \cdot \frac{\boldsymbol{g} - \hat{\boldsymbol{g}}}{\sqrt{1 + \|\boldsymbol{g}\|^2}} \\ =& \Gamma'_g(\hat{\boldsymbol{g}}) \cdot \frac{\boldsymbol{g} - \hat{\boldsymbol{g}}}{\sqrt{1 + \|\boldsymbol{g}\|^2}} \end{aligned} \tag{73}$$

This new form is obtained through the following identity:

$$1 + \boldsymbol{g} \cdot \hat{\boldsymbol{g}} = \sqrt{\frac{(1 + \|\hat{\boldsymbol{g}}\|^2)(1 + \|\boldsymbol{g}\|^2)}{(1 + \|\boldsymbol{g}^+\|^2)}} \tag{74}$$

Note that Eq. (73) is an exact relationship. It can also be rewritten as

$$\boldsymbol{q}^+_{1:3} = \Gamma'_g(\hat{\boldsymbol{g}}) \left(\boldsymbol{q}_{1:3} - \frac{q_4}{\hat{q}_4} \hat{\boldsymbol{q}}_{1:3} \right) \tag{75}$$

which is equivalent to Eq. (37), also an exact relationship.

The alternative attitude error-covariance reset matrix is related to $\Gamma_g(\hat{\boldsymbol{g}})$ and $\Gamma_q(\hat{\boldsymbol{q}}_{1:3})$ through

$$\Gamma'_g(\hat{\boldsymbol{g}}) = \sqrt{1 + \|\hat{\boldsymbol{g}}\|^2} \;\; \Gamma_g(\hat{\boldsymbol{g}}) \tag{76}$$

and

$$\begin{aligned} \Gamma'_g(\hat{\boldsymbol{g}}) &= [I_3 \quad \boldsymbol{0}_{3\times 1}] \;\; \Xi(\hat{\boldsymbol{q}}) \\ &= \Gamma_q(\hat{\boldsymbol{q}}_{1:3}) - \frac{\hat{\boldsymbol{q}}_{1:3}\hat{\boldsymbol{q}}^T_{1:3}}{\sqrt{1 - \|\hat{\boldsymbol{q}}_{1:3}\|^2}} \end{aligned} \tag{77}$$

respectively, where $\boldsymbol{0}_{3\times 1}$ denotes a 3×1 vector of zeros. The matrix in terms of the Euler axis and angle is given by

$$\begin{aligned} \Gamma'_g(\hat{\boldsymbol{e}}, \hat{\vartheta}) &= \cos(\hat{\vartheta}/2) I_3 - \sin(\hat{\vartheta}/2)[\hat{\boldsymbol{e}}\times] \\ &= A(\hat{\boldsymbol{e}}, \hat{\vartheta}/2) H'_g(\hat{\boldsymbol{e}}, \hat{\vartheta}) \end{aligned} \tag{78}$$

where $H'_g(\hat{\boldsymbol{e}}, \hat{\vartheta})$ is a symmetric matrix given by

$$H'_g(\hat{\boldsymbol{e}}, \hat{\vartheta}) = \hat{\boldsymbol{e}}\hat{\boldsymbol{e}}^T \cos(\hat{\vartheta}/2) + \left(I_3 - \hat{\boldsymbol{e}}\hat{\boldsymbol{e}}^T \right) \tag{79}$$

The three eigenvalues of $H'_g(\hat{\boldsymbol{e}}, \hat{\vartheta})$ are 1, 1, and $\cos(\hat{\vartheta}/2)$.

VI. Brief Discussion

The three-component attitude error vector $\boldsymbol{\delta}$ in all the attitude error parameterizations considered so far is the product of the Euler rotation axis $\boldsymbol{e}$ and a scalar function of the Euler rotation angle ϑ, and it approaches the limit $\boldsymbol{\delta} \approx \boldsymbol{\vartheta}/n$ for some integer n as ϑ approaches zero. The reset of the attitude error in all these parameterizations takes the form

$$\boldsymbol{\delta}^+ = \Gamma_\delta(\hat{\boldsymbol{\delta}})\boldsymbol{\Delta\delta} \tag{80}$$

Except for $\Gamma'_g(\hat{\boldsymbol{g}})$, $\Gamma_\delta(\boldsymbol{\delta})$ is the matrix appearing in the kinematic relation

$$\boldsymbol{\omega} = n\Gamma_\delta(\boldsymbol{\delta})\dot{\boldsymbol{\delta}} \tag{81}$$

as can be seen by comparison with Eqs. (3.21), (3.23), (3.25), and (3.30) in [12].

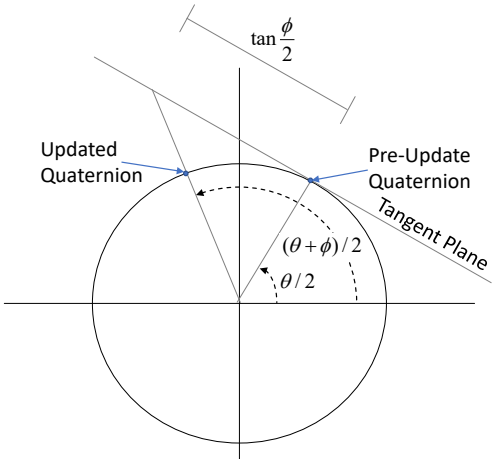

Fig. 1 Tangent plane with pre-update and post-update quaternions.

All of these resets are the same to first order in the attitude update, so the choice of attitude parameterization does not have any significant effect on the error-covariance reset if the update is small enough, as is usually the case where the EKF is applicable. To first order, all the resets rotate errors by half the angle of the update about the axis of the update. Why the half-angle appears, even for the rotation vector parameterization that does not seem *a priori* to involve half-angles at all, is something of a mystery. One possible explanation is given by looking at Fig. 1, which indicates that the reset is a mapping from the tangent space of the pre-update quaternion to the post-update quaternion. Those two tangent spaces are a separated by the half angle. The different parameterizations generally change the magnitudes of the errors parallel and perpendicular to the attitude update by different scale factors, but all the magnitude changes are of second or higher order in the size of the attitude update. The changes to the 2-norm of the attitude error-covariance

matrix P_δ are given by

$$\cos^2(\hat{\vartheta}/2)\cdot\|P_\delta\|_2 \le \left\|\Gamma'_g(\hat{\boldsymbol{g}})\,P_\delta\,(\Gamma'_g(\hat{\boldsymbol{g}}))^T\right\|_2 \le \|P_\delta\|_2 \tag{82a}$$

$$\cos^4(\hat{\vartheta}/2)\cdot\|P_\delta\|_2 \le \left\|\Gamma_g(\hat{\boldsymbol{g}})\,P_\delta\,\Gamma_g^T(\hat{\boldsymbol{g}})\right\|_2 \le \cos^2(\hat{\vartheta}/2)\cdot\|P_\delta\|_2 \tag{82b}$$

$$\|P_\delta\|_2 \le \left\|\Gamma_q(\hat{\boldsymbol{q}}_{1:3})\,P_\delta\,\Gamma_q^T(\hat{\boldsymbol{q}}_{1:3})\right\|_2 \le \cos^{-2}(\hat{\vartheta}/2)\cdot\|P_\delta\|_2 \tag{82c}$$

$$(4/\hat{\vartheta}^2)\sin^2(\hat{\vartheta}/2)\cdot\|P_\delta\|_2 \le \left\|\Gamma_\vartheta(\hat{\boldsymbol{\vartheta}})\,P_\delta\,\Gamma_\vartheta^T(\hat{\boldsymbol{\vartheta}})\right\|_2 \le \|P_\delta\|_2 \tag{82d}$$

where $\|\cdot\|$ denotes the 2-norm of a matrix, and $\left\|\Gamma_p(\hat{\boldsymbol{p}})\,P_\delta\,\Gamma_p^T(\hat{\boldsymbol{p}})\right\|_2 = \cos^4(\hat{\vartheta}/4)\cdot\|P_\delta\|_2$. Small attitude updates result in small difference between P_δ and $\Gamma_\delta(\hat{\boldsymbol{\delta}})P_\delta\Gamma_\delta^T(\hat{\boldsymbol{\delta}})$, but the difference is not negligible for large attitude updates. Whether the error-covariance reset is necessary can be determined based on the magnitude $\hat{\vartheta}$ of the attitude update.

It is easy to say that one should not be using any kind of an EKF if the attitude updates are large, but it would be desirable to have robustness and global stability in the presence of large errors. Therefore, the performance of the various resets in two test cases with large errors is now investigated. The different approximations in the linearizations used to compute the various Γ matrices can be expected to result in different performance.

VII. Test Cases

First consider a parallel-axis case with $\boldsymbol{\vartheta} = \pi\boldsymbol{e}$ and $\hat{\boldsymbol{\vartheta}} = (2\pi/3)\boldsymbol{e}$. In this case the exact reset is $\vartheta^+_{\text{exact}} = \|\boldsymbol{\vartheta} - \hat{\boldsymbol{\vartheta}}\| = \|\Delta\boldsymbol{\vartheta}\| = \pi/3 = 60^\circ$. The linearized resets are

$$\sin\left(\vartheta_q^+/2\right) = [\sin(\vartheta/2) - \sin(\hat{\vartheta}/2)]/\cos(\hat{\vartheta}/2) = 2 - \sqrt{3}, \qquad \vartheta_q^+ = 31.1^\circ \tag{83a}$$

$$\tan\left(\vartheta_g^+/2\right) = \cos^2(\hat{\vartheta}/2)[\tan(\vartheta/2) - \tan(\hat{\vartheta}/2)] = \infty, \qquad \vartheta_g^+ = 180^\circ \tag{83b}$$

$$\tan\left(\vartheta_p^+/4\right) = \cos^2(\hat{\vartheta}/4)[\tan(\vartheta/4) - \tan(\hat{\vartheta}/4)] = (3 - \sqrt{3})/4, \qquad \vartheta_p^+ = 70.4^\circ \tag{83c}$$

$$\vartheta_\vartheta^+ = \vartheta - \hat{\vartheta}, \qquad \vartheta_\vartheta^+ = 60^\circ \tag{83d}$$

The magnitude of ϑ_ϑ^+ is exact, as is found before, and the MRP reset is reasonably close, but the quaternion reset is much too small, and the Rodrigues-Gibbs reset is much too large.

Now consider a case with $\boldsymbol{\vartheta} = (\pi/2)\boldsymbol{e}, \hat{\boldsymbol{\vartheta}} = (\pi/2)\hat{\boldsymbol{e}}$, and $\boldsymbol{e}\cdot\hat{\boldsymbol{e}} = 0$. These values are chosen to give an analytically tractable model having an attitude error with the very large magnitude $\|\Delta\boldsymbol{\vartheta}\| = (\pi/2)\|\boldsymbol{e} - \hat{\boldsymbol{e}}\| = \pi/\sqrt{2} = 127.3^\circ$. Equations (54) and (55) give the exact $\boldsymbol{\vartheta}^+$ in terms of

$$\boldsymbol{w} = \frac{\sqrt{3}}{2}\frac{\boldsymbol{e} - \hat{\boldsymbol{e}} + \boldsymbol{e}\times\hat{\boldsymbol{e}}}{\sqrt{3}} = \sin(\pi/3)\frac{\boldsymbol{e} - \hat{\boldsymbol{e}} + \boldsymbol{e}\times\hat{\boldsymbol{e}}}{\sqrt{3}} \tag{84}$$

where the separation into a magnitude and a unit vector has been shown explicitly. Then

$$\boldsymbol{\vartheta}^+_{\text{exact}} = \vartheta^+_{\text{exact}}\, \boldsymbol{e}^+_{\text{exact}} = \frac{2\pi}{3} \cdot \frac{\boldsymbol{e} - \hat{\boldsymbol{e}} + \boldsymbol{e} \times \hat{\boldsymbol{e}}}{\sqrt{3}} \tag{85}$$

The vector $\boldsymbol{\vartheta}^+_{\text{exact}}$ is obtained by rotating $\boldsymbol{\Delta\vartheta}$ by an angle $\pi/4$ around $\hat{\boldsymbol{e}}$, compressing the component parallel to $\hat{\boldsymbol{e}}$ by a factor by $\sqrt{16/27} = 0.77$, and stretching the components perpendicular to $\hat{\boldsymbol{e}}$ by a factor $\sqrt{32/27} = 1.09$.

The linearized resets in this case give

$$\boldsymbol{q}^+_{1:3} = \sin(\vartheta^+_q/2)\boldsymbol{e}^+_q = \Gamma_q(\hat{\boldsymbol{q}}^+_{1:3})\frac{1}{\sqrt{2}}(\boldsymbol{e} - \hat{\boldsymbol{e}}) = \frac{\sqrt{6}}{2}\frac{\boldsymbol{e} - 2\hat{\boldsymbol{e}} + \boldsymbol{e} \times \hat{\boldsymbol{e}}}{\sqrt{6}}, \qquad \sin(\vartheta^+_q/2) > 1 \tag{86a}$$

$$\boldsymbol{g}^+ = \tan(\vartheta^+_g/2)\boldsymbol{e}^+_g = \Gamma_g(\hat{\boldsymbol{g}})(\boldsymbol{e} - \hat{\boldsymbol{e}}) = \frac{\sqrt{3}}{2}\frac{\boldsymbol{e} - \hat{\boldsymbol{e}} + \boldsymbol{e} \times \hat{\boldsymbol{e}}}{\sqrt{3}}, \qquad \vartheta^+_g = 81.8^\circ \tag{86b}$$

$$\boldsymbol{p}^+ = \tan(\vartheta^+_p/4)\boldsymbol{e}^+_p = \Gamma_p(\hat{\boldsymbol{p}})(\sqrt{2} - 1)(\boldsymbol{e} - \hat{\boldsymbol{e}}) = \frac{1}{2}\frac{\boldsymbol{e} - \sqrt{2}\hat{\boldsymbol{e}} + \boldsymbol{e} \times \hat{\boldsymbol{e}}}{2}, \qquad \vartheta^+_p = 106.3^\circ \tag{86c}$$

$$\boldsymbol{\vartheta}^+ = \vartheta^+_{\vartheta}\boldsymbol{e}^+_{\vartheta} = \Gamma_{\vartheta}(\hat{\boldsymbol{\vartheta}})\frac{\pi}{2}(\boldsymbol{e} - \hat{\boldsymbol{e}}) = \sqrt{(\pi/2)^2 + 2}\frac{\boldsymbol{e} - (\pi/2)\hat{\boldsymbol{e}} + \boldsymbol{e} \times \hat{\boldsymbol{e}}}{\sqrt{(\pi/2)^2 + 2}}, \qquad \vartheta^+_{\vartheta} = 121.1^\circ \tag{86d}$$

These resets are in agreement with rotation by angle $\pi/4$ around $\hat{\boldsymbol{e}}$ and stretching by the factors that have been found previously of the components parallel and perpendicular to $\hat{\boldsymbol{e}}$. They all give approximately the correct direction $\boldsymbol{e}^+$, specifically $\boldsymbol{e}^+_q \cdot \boldsymbol{e}^+_{\text{exact}} = \cos(19.5^\circ)$, $\boldsymbol{e}^+_g = \boldsymbol{e}^+_{\text{exact}}$, $\boldsymbol{e}^+_p \cdot \boldsymbol{e}^+_{\text{exact}} = \cos(9.7^\circ)$, and $\boldsymbol{e}^+_{\vartheta} \cdot \boldsymbol{e}^+_{\text{exact}} = \cos(12.7^\circ)$. The magnitude of $\vartheta^+_{\vartheta}$is very close to the exact value of 120°, but the quaternion reset is too large, and the Rodrigues-Gibbs and MRP resets are too small. The especially small value of the Rodrigues-Gibbs reset for this test case can be understood by inspection of Eq. (23). The term $\boldsymbol{g} \cdot \hat{\boldsymbol{g}}$ in the denominator is zero in the exact computation, but it is set to $\|\hat{\boldsymbol{g}}\|^2 = 1$ in the linearization.

Finding $\left\|\boldsymbol{q}^+_{1:3}\right\| > 1$ is a conceptual problem, but not a computational problem, because $\boldsymbol{q}^+_{1:3}$ is only used to compute the reset error-covariance and not to compute any attitude. An attitude update with $\|\hat{\boldsymbol{q}}_{1:3}\| > 1$ would lead to an imaginary value of $\hat{q}_4$, though. Truncating $\hat{\boldsymbol{q}}_{1:3}$ could avoided this, but would result in a biased estimate with $E\left\{\boldsymbol{q}^+_{1:3}\right\} \neq \boldsymbol{0}$. It should be pointed out that no three-parameter global attitude parameterization is without problems [8]. The Rodrigues-Gibbs vector becomes infinite as the rotation approaches 180°. The MRP and rotation vector parameterizations have a "wrapping" problem. A computed $\|\hat{\boldsymbol{p}}\| > 1$ or $\|\hat{\boldsymbol{\vartheta}}\| > \pi$ calls for an angle correction larger than 180°, which is actually equivalent to a smaller rotation angle. These parameterizations could handle such large $\boldsymbol{\delta}$ updates without infinities, truncations, divisions by zero, or square roots of negative numbers, but the reference attitude and error-covariance resets would not be correct.

VIII. Linear Measurement Model

A linear measurement model that improves the convergence properties of the MEKF [13] is reviewed. The vector measurement model is given by

$$\tilde{\boldsymbol{b}}_i = A(\boldsymbol{q})\boldsymbol{r}_i + \boldsymbol{\nu}_i'' \tag{87}$$

where $\boldsymbol{q}$ is the true attitude quaternion, $\tilde{\boldsymbol{b}}_i$ is the ith measured vector in the body frame, and $\boldsymbol{r}_i$ is the ith known reference vector in the reference frame. Note that in this section, $\boldsymbol{q}$ represents the global attitude, not the local attitude errors. The measurement noise $\boldsymbol{\nu}_i$ satisfies $E\{\boldsymbol{\nu}_i\} = \mathbf{0}_{3\times 1}$, and $E\{\boldsymbol{\nu}_i''(\boldsymbol{\nu}_i'')^T\} = (\sigma_i')^2 I_3$. With unit vectors $\tilde{\hat{\boldsymbol{b}}}_i = \tilde{\boldsymbol{b}}_i/\|\tilde{\boldsymbol{b}}_i\|$ and $\hat{\boldsymbol{r}}_i = \boldsymbol{r}_i/\|\boldsymbol{r}_i\|$, the measurement model becomes

$$\tilde{\hat{\boldsymbol{b}}}_i = A(\boldsymbol{q})\hat{\boldsymbol{r}}_i + \boldsymbol{\nu}_i' \tag{88}$$

with $E\{\boldsymbol{\nu}_i'(\boldsymbol{\nu}_i')^T\} = \sigma_i^2(I_3 - \hat{\boldsymbol{b}}_i\hat{\boldsymbol{b}}_i^T)$ [20], where

$$\hat{\boldsymbol{b}}_i = A(\boldsymbol{q})\hat{\boldsymbol{r}}_i \tag{89}$$

The exact linear measurement model is based on Eq. (89) and

$$A(\boldsymbol{q}) = A(\boldsymbol{g})A(\bar{\boldsymbol{q}}) \tag{90}$$

where $\bar{\boldsymbol{q}}$ denotes the pre-update quaternion estimate and $\boldsymbol{g}$ denotes the Rodrigues-Gibbs vector for attitude errors. Equation (89) can be rewritten as [13]

$$\mathcal{N}_i\boldsymbol{q} = \mathbf{0}_{4\times 1} \tag{91}$$

or

$$N_i^T\boldsymbol{q} = \mathbf{0}_{2\times 1} \tag{92}$$

The rank–2, 4×4 matrix $\mathcal{N}_i$ is given by

$$\mathcal{N}_i = \frac{1}{2}\begin{bmatrix} (1+\hat{\boldsymbol{r}}_i^T\hat{\boldsymbol{b}}_i)I_3 - \hat{\boldsymbol{r}}_i\hat{\boldsymbol{b}}_i^T - \hat{\boldsymbol{b}}_i\hat{\boldsymbol{r}}_i^T & \hat{\boldsymbol{r}}_i\times\hat{\boldsymbol{b}}_i \\ (\hat{\boldsymbol{r}}_i\times\hat{\boldsymbol{b}}_i)^T & 1-\hat{\boldsymbol{r}}_i^T\hat{\boldsymbol{b}}_i \end{bmatrix} \tag{93}$$

and the 4×2 matrix N_i satisfies

$$N_iN_i^T = \mathcal{N}_i \tag{94}$$

$$N_i^TN_i = I_2 \tag{95}$$

Equation (90) is equivalent to

$$\boldsymbol{q} = \frac{\bar{\boldsymbol{q}} + \Xi(\bar{\boldsymbol{q}})\boldsymbol{g}}{\sqrt{1 + \|\boldsymbol{g}\|^2}} \tag{96}$$

Substituting Eq. (96) into Eq. (92) gives an exact linear model in $2\boldsymbol{g}$:

$$-2N_i^T \bar{\boldsymbol{q}} = N_i^T \Xi(\boldsymbol{q})\ (2\boldsymbol{g}) \tag{97}$$

The linear measurement model follows from the exact model

$$\tilde{\boldsymbol{y}}_i = \tilde{H}_i \Delta\boldsymbol{x} + \boldsymbol{\nu}_i \tag{98}$$

where $\Delta\boldsymbol{x} = [2\boldsymbol{g}^T \quad \boldsymbol{\beta}^T]^T$, and

$$\tilde{\boldsymbol{y}}_i = -2\tilde{N}_i^T \bar{\boldsymbol{q}} \tag{99a}$$

$$\tilde{H}_i = \begin{bmatrix} \tilde{N}_i^T \Xi(\bar{\boldsymbol{q}}) & 0_{2\times(m-3)} \end{bmatrix} \tag{99b}$$

$$\tilde{N}_i \tilde{N}_i^T = \tilde{\mathcal{N}}_i, \quad \tilde{N}_i^T \tilde{N}_i = I_2 \tag{99c}$$

$$\tilde{\mathcal{N}}_i = \frac{1}{2}\begin{bmatrix} (1 + \hat{\boldsymbol{r}}_i^T \tilde{\hat{\boldsymbol{b}}}) I_3 - \hat{\boldsymbol{r}}_i \tilde{\hat{\boldsymbol{b}}}^T - \tilde{\hat{\boldsymbol{b}}} \hat{\boldsymbol{r}}_i^T & \hat{\boldsymbol{r}}_i \times \tilde{\hat{\boldsymbol{b}}} \\ (\hat{\boldsymbol{r}}_i \times \tilde{\hat{\boldsymbol{b}}})^T & 1 - \hat{\boldsymbol{r}}_i^T \tilde{\hat{\boldsymbol{b}}} \end{bmatrix} \tag{99d}$$

It is now shown that $E\{\boldsymbol{\nu}_i \boldsymbol{\nu}_i^T\} \approx \sigma_i^2 I_2$. Let $\delta\mathcal{N}_i = \tilde{\mathcal{N}}_i - \mathcal{N}_i$. Substituting $\mathcal{N}_i = \tilde{\mathcal{N}}_i - \delta\mathcal{N}_i$ into Eq. (91) gives

$$-2\tilde{\mathcal{N}}_i \boldsymbol{q} = -2\delta\mathcal{N}_i\ \boldsymbol{q} \tag{100}$$

Denoting the right-hand side noise term by $\boldsymbol{\gamma}_i$ gives

$$-2\tilde{\mathcal{N}}_i \boldsymbol{q} = \boldsymbol{\gamma}_i \tag{101}$$

Clearly, $\boldsymbol{\gamma}_i$ is linear in $\boldsymbol{\nu}_i'$. It can be verified that

$$\begin{aligned} \boldsymbol{\gamma}_i =& -2\delta\mathcal{N}_i\ \boldsymbol{q} \\ =& \tilde{\mathcal{H}}_i\ \Xi(\boldsymbol{q})\ \boldsymbol{\nu}_i' \\ =& \mathcal{H}_i\ \Xi(\boldsymbol{q})\ \boldsymbol{\nu}_i' + \frac{1}{2}\Omega^2(\boldsymbol{\nu}_i')\boldsymbol{q} \\ \approx& \mathcal{H}_i\ \Xi(\boldsymbol{q})\ \boldsymbol{\nu}_i' \end{aligned} \tag{102}$$

where

$$\Omega(\boldsymbol{b}) = \begin{bmatrix} -[\boldsymbol{b}\times] & \boldsymbol{b} \\ -\boldsymbol{b}^T & 0 \end{bmatrix} \tag{103}$$

and

$$\tilde{\mathcal{H}}_i = -\tilde{\mathcal{H}}_i^T = \frac{1}{2}\begin{bmatrix} -\left[(\tilde{\hat{\boldsymbol{b}}}_i + \hat{\boldsymbol{r}}_i)\times\right] & \tilde{\hat{\boldsymbol{b}}}_i - \hat{\boldsymbol{r}}_i \\ -\left(\tilde{\hat{\boldsymbol{b}}}_i - \hat{\boldsymbol{r}}_i\right)^T & 0 \end{bmatrix} \tag{104}$$

$$\mathcal{H}_i = -\mathcal{H}_i^T = \frac{1}{2}\begin{bmatrix} -\left[(\hat{\boldsymbol{b}}_i + \hat{\boldsymbol{r}}_i)\times\right] & \hat{\boldsymbol{b}}_i - \hat{\boldsymbol{r}}_i \\ -\left(\hat{\boldsymbol{b}}_i - \hat{\boldsymbol{r}}_i\right)^T & 0 \end{bmatrix} \tag{105}$$

The matrices $\tilde{\mathcal{H}}_i$ and $\mathcal{H}_i$ satisfy

$$\tilde{\mathcal{H}}_i\tilde{\mathcal{H}}_i^T = \tilde{\mathcal{H}}_i^T\tilde{\mathcal{H}}_i = -\tilde{\mathcal{H}}_i\,\Omega\left(\tilde{\hat{\boldsymbol{b}}}_i\right) = \tilde{\mathcal{N}}_i \tag{106}$$

$$\mathcal{H}_i\mathcal{H}_i^T = \mathcal{H}_i^T\mathcal{H}_i = -\mathcal{H}_i\,\Omega\left(\hat{\boldsymbol{b}}_i\right) = \mathcal{N}_i \tag{107}$$

From Eq. (102), the mean $E\{\boldsymbol{\gamma}_i\} \approx \mathbf{0}_{4\times1}$, and the covariance of $\boldsymbol{\gamma}_i$ is given by

$$\begin{aligned} E\left\{\boldsymbol{\gamma}_i\boldsymbol{\gamma}_i^T\right\} &\approx \mathcal{H}_i\,\Xi(\boldsymbol{q})\,E\left\{\boldsymbol{\nu}_i'(\boldsymbol{\nu}_i')^T\right\}\Xi^T(\boldsymbol{q})\mathcal{H}_i^T \\ &= \sigma_i^2\mathcal{H}_i\,\Xi(\boldsymbol{q})\left(I_3 - \hat{\boldsymbol{b}}_i\hat{\boldsymbol{b}}_i^T\right)\Xi^T(\boldsymbol{q})\mathcal{H}_i^T \end{aligned} \tag{108}$$

Using the identities $\Xi(\boldsymbol{q})\Xi^T(\boldsymbol{q}) = I_4 - \boldsymbol{q}\boldsymbol{q}^T$, $\Xi(\boldsymbol{q})\hat{\boldsymbol{b}}_i = \Omega(\hat{\boldsymbol{b}}_i)\boldsymbol{q}$, $\mathcal{H}_i\,\Omega\left(\hat{\boldsymbol{b}}_i\right) = -\mathcal{N}_i$, and $\mathcal{H}_i\mathcal{H}_i^T = \mathcal{N}_i$ yields

$$\begin{aligned} E\left\{\boldsymbol{\gamma}_i\boldsymbol{\gamma}_i^T\right\} &\approx \sigma_i^2\mathcal{N}_i - \sigma_i^2\left[\mathcal{H}_i\boldsymbol{q}\boldsymbol{q}^T\mathcal{H}_i^T + \mathcal{N}_i\boldsymbol{q}\boldsymbol{q}^T\mathcal{N}_i^T\right] \\ &= \sigma_i^2\mathcal{N}_i \end{aligned} \tag{109}$$

Pre-multiplying Eq. (101) by $\tilde{N}_i^T$ gives

$$-2\tilde{N}_i^T\boldsymbol{q} = \tilde{N}_i^T\gamma_i \tag{110}$$

where $\tilde{N}_i^T\tilde{\mathcal{N}}_i = \tilde{N}_i^T(\tilde{N}_i\tilde{N}_i^T) = (\tilde{N}_i^T\tilde{N}_i)\tilde{N}_i^T = \tilde{N}_i^T$ has been used. Substituting Eq. (96) into Eq. (110) gives

$$-2\tilde{N}_i^T\frac{\bar{\boldsymbol{q}} + \Xi(\bar{\boldsymbol{q}})\boldsymbol{g}}{\sqrt{1 + \|\boldsymbol{g}\|^2}} = \tilde{N}_i^T\gamma_i \tag{111}$$

Multiplying both sides by $\sqrt{1+\|\boldsymbol{g}\|^2}$ and rearranging terms gives

$$-2\tilde{N}_i^T\bar{\boldsymbol{q}} = 2\tilde{N}_i^T\Xi(\bar{\boldsymbol{q}})\boldsymbol{g} + \sqrt{1+\|\boldsymbol{g}\|^2}\;\tilde{N}_i^T\gamma_i \tag{112}$$

Comparing it with Eq. (98) shows

$$\boldsymbol{\nu}_i = \sqrt{1+\|\boldsymbol{g}\|^2}\;\tilde{N}_i^T\gamma_i \tag{113}$$

Hence,

$$E\{\boldsymbol{\nu}_i\boldsymbol{\nu}_i^T\} = (1+\|\boldsymbol{g}\|^2)E\left\{\tilde{N}_i^T\boldsymbol{\gamma}_i\boldsymbol{\gamma}_i^T\tilde{N}_i\right\} \tag{114}$$

Ignoring higher than second-order terms yields

$$\begin{aligned} E\left\{\tilde{N}_i^T\boldsymbol{\gamma}_i\boldsymbol{\gamma}_i^T\tilde{N}_i\right\} &\approx N_i^T E\left\{\boldsymbol{\gamma}_i\boldsymbol{\gamma}_i^T\right\}N_i \\ &= \sigma_i^2 N_i^T \mathcal{N}_i N_i \\ &= \sigma_i^2 I_2 \end{aligned} \tag{115}$$

Hence,

$$E\{\boldsymbol{\nu}_i\boldsymbol{\nu}_i^T\} \approx (1+\|\boldsymbol{g}\|^2)\sigma_i^2 I_2 \tag{116}$$

For small $\boldsymbol{g}$,

$$E\{\boldsymbol{\nu}_i\boldsymbol{\nu}_i^T\} \approx \sigma_i^2 I_2 \tag{117}$$

IX. Error-Covariance Reset in the Kalman and Unscented Filters

Assume that the m-dimensional error-state vector is $\boldsymbol{\Delta x} = [n\boldsymbol{\delta}^T \;\; \boldsymbol{\Delta\beta}^T]^T$, where $n\boldsymbol{\delta}$ denotes the full-angle attitude-error vector and may be interpreted as $2\boldsymbol{g}$, $2\boldsymbol{q}_{1:3}$, $4\boldsymbol{p}$, or $\boldsymbol{\vartheta}$, and $\boldsymbol{\Delta\beta}$ denotes the vector of other variables to be estimated. Assume also that the $m\times m$ pre-reset and post-reset error-covariance matrices associated with the error state are $P_{\Delta x}$ and $P_{\Delta x}^+$, respectively. Five attitude and error-covariance reset schemes are considered, from zeroth-order to second-order. In all but the last one, the global attitude estimate is updated by Eq. (20): $\hat{A}^+ = A(\hat{\boldsymbol{\delta}})\hat{A}$.

The zeroth-order error-covariance reset is simply no reset: $P_{\Delta x}^+ = P_{\Delta x}$. The first-order error-covariance reset is carried out by a linear transformation based on the $\Gamma_\delta(\hat{\boldsymbol{\delta}})$ matrix:

$$P_{\Delta x}^+ = \begin{bmatrix} \Gamma_\delta(\hat{\boldsymbol{\delta}}) & 0_{3\times(m-3)} \\ 0_{(m-3)\times 3} & I_{(m-3)} \end{bmatrix} P_{\Delta x} \begin{bmatrix} \Gamma_\delta(\hat{\boldsymbol{\delta}}) & 0_{3\times(m-3)} \\ 0_{(m-3)\times 3} & I_{(m-3)} \end{bmatrix}^T \tag{118}$$

where $0_{p\times q}$ is a $p\times q$ matrix of zeros. The first-order error-covariance reset reduces to the zeroth-order error-covariance

reset if $\Gamma_\delta(\hat{\boldsymbol{\delta}}) = I_3$, which is a good approximation under the small angle assumption.

Owing to the complexity with analytical expressions, the three second-order attitude and error-covariance resets are implemented numerically with the Unscented Transform (UT) [21]. The implementation of the UT for the error-covariance reset is based on that of [22]. The nonlinear function to which the UT is applied is the mapping from the pre-reset error state $\boldsymbol{\Delta x}$ to the post-reset error state $\boldsymbol{\Delta x}^+$, where $\boldsymbol{\Delta x}$ is assumed to be a zero-mean Gaussian random vector with covariance $P_{\Delta x}$, $\boldsymbol{\Delta\beta}^+ = \boldsymbol{\Delta\beta}$, but the mapping from $\boldsymbol{\delta}$ to $\boldsymbol{\delta}^+$ is nonlinear.

In the first second-order reset (UT1), the nonlinear mapping from $\boldsymbol{\delta}$ to $\boldsymbol{\delta}^+$ is implicitly defined by Eq. (22): $A\left(\boldsymbol{\delta}^+\right) = A(\boldsymbol{\delta})\, A^{-1}(\hat{\boldsymbol{\delta}})$. The post-reset mean $\hat{\boldsymbol{\delta}}^+$ is computed with the UT under the Gaussian assumption for $\boldsymbol{\delta}$. Note that $\hat{\boldsymbol{\delta}}^+ = \mathbf{0}_{3\times1}$ is valid to first order only. The other two second-order error-covariance resets reduce the bias in $\hat{\boldsymbol{\delta}}^+$ by using

$$A\left(\boldsymbol{\delta}^+\right) = A(\boldsymbol{\delta})\, A^{-1}(\hat{\boldsymbol{\delta}}^*) \tag{119}$$

where $\hat{\boldsymbol{\delta}}^*$ is sought such that $\hat{\boldsymbol{\delta}}^+ = \mathbf{0}_{3\times1}$ is valid to second order. The post-reset mean $\hat{\boldsymbol{\delta}}^+$ corresponding to $\hat{\boldsymbol{\delta}}^*$ is numerically determined using the UT. A simple iterative optimization process for the variable $\hat{\boldsymbol{\delta}}^*$ is used to yield a result that is as close to being zero-mean possible. The second second-order reset (UT2) updates the global attitude estimate using $\hat{A}^+ = A(\hat{\boldsymbol{\delta}})\hat{A}$. The last second-order reset (UT3) updates the global attitude estimate using $\hat{A}^+ = A(\hat{\boldsymbol{\delta}}^*)\hat{A}$.

The error-covariance reset can also be used with other filters. An iterated EKF for attitude estimation is shown in [23]. The error-covariance reset will be done at the end of the iterations for this filter. The particle filter shown in [24] does not use the error-covariance because it estimates the entire probability density using weighted particle states. However, other particle filter formulations approximate the optimal importance density by incorporating the current measurement with an EKF or an Unscented filter [25]. These localized particle filters can use the error-covariance reset shown in this section.

X. Numerical Simulations

To compare the error-covariance resets of different orders and understand the efficacy of the linear measurement model, full attitude filters are compared through the simulation example of [22], which simulates the Tropical Rainfall Measuring Mission spacecraft, which was an Earth-pointing spacecraft in a near-circular 90 min (350 km) orbit with an inclination of 35°. The nominal Earth-pointing mission mode requires a rotation once per orbit about the spacecraft's y-axis. The attitude determination hardware consists of an Earth sensor assembly, digital Sun sensors, coarse Sun sensors, a three-axis magnetometer (TAM), and gyroscopic rate sensors. In the simulations, only TAM and gyro measurements are used. The data span is 8 hr. For the details of the TAM and gyro measurements, see [22].

The simulation example of [22] includes three single-run cases. They share the TAM and gyro measurements but differ in the initial estimation errors and the associated initial error-covariance. The true initial gyro biases are

0.1 deg/hr on each axis in all the cases. In Case 1, the initial attitude errors are set to zero. The initial bias estimate is set to zero; hence, the initial bias errors are 0.1 deg/hr on each axis. The initial attitude error-covariance is given by $P_{\text{att}} = (0.5 \text{ deg})^2 I_3$, and the initial bias error-covariance is given by $P_{\text{bias}} = (0.2 \text{ deg/hr})^2 I_3$. In Case 2, the initial attitude error quaternion is $[0, 0, 1, 1]^T/\sqrt{2}$, which corresponds to an attitude error of 90 deg. The initial bias estimate remains zero. The initial error-covariances are set to $10000P_{\text{att}}$ and P_{bias}, respectively. In Case 3, the initial attitude errors are the same as Case 2, but the initial y-axis bias estimate also increases to 20 deg/hr. The initial error-covariances are $10000P_{\text{att}}$ and $10000P_{\text{bias}}$. A 100-run Monte Carlo simulation (Case 4) is added, where the initial bias estimate and error-covariance are the same as in Cases 1 and 2, but the attitude errors are randomly generated according to the error-covariance $3600P_{\text{att}}$.

Two tests are run and the results are presented in the two subsections that follow. The first test includes all four cases and up to second-order error-covariance resets. All the filters use the measurement model given by Eq. (87). The second test is focused on Case 3 only, where the linear measurement model given by Eq. (98) is used and the linear error-covariance resets are compared.

A. Error-Covariance Resets of Difference Orders

The zeroth-, first-, and second-order reset schemes are incorporated into the MEKF and UnScented QUaternion Estimator (USQUE) [22], a multiplicative Unscented filter, to form ten filters. The Unscented filter is closely related to a second-order EKF, while the standard EKF is a first-order filter [26]. The ten filters are respectively labeled "MEKF," "MEKF RESET," "MEKF RESET UT1," "MEKF RESET UT2," "MEKF RESET UT3," "USQUE," "USQUE RESET," "USQUE RESET UT1," "USQUE RESET UT2," and "USQUE RESET UT3." The five MEKFs are identical except for the reset operation. So are the five USQUEs.

Plots of the attitude errors are shown in Figs. 2–5. The corresponding root mean square errors (RMSE) over the entire eight hours and over the last four hours are shown in Tables 1–4. The former includes the transient and "steady-state" errors; the latter is largely the "steady-state" error.

Figure 2 and Table 1 show that in Case 1, the differences among the filters, if any, are hardly discernible. The RMSE of 0.0036 deg over the last four hours approximately represents the attainable attitude estimation accuracy from the 8-hr dataset. Furthermore, almost identical results are obtained when the initial attitude errors are set to 5 deg on each axis. All these results support the conviction that when the attitude errors are small, the error-covariance reset has negligible effects on the convergence and accuracy of the filters.

The MEKF is known to suffer slow convergence in Case 2 and to diverge in Case 3. Figure 3 and Table 2 show that the first-order reset does not improve the convergence rate of the MEKF. Figure 4 and Table 3 show that it does not prevent the MEKF from diverging, either. The second-order resets, however, improve the MEKF in both the convergence rate and accuracy. Note that in Figs. 3 and 4, the curves for the MEKF with second-order error-covariance resets tend to

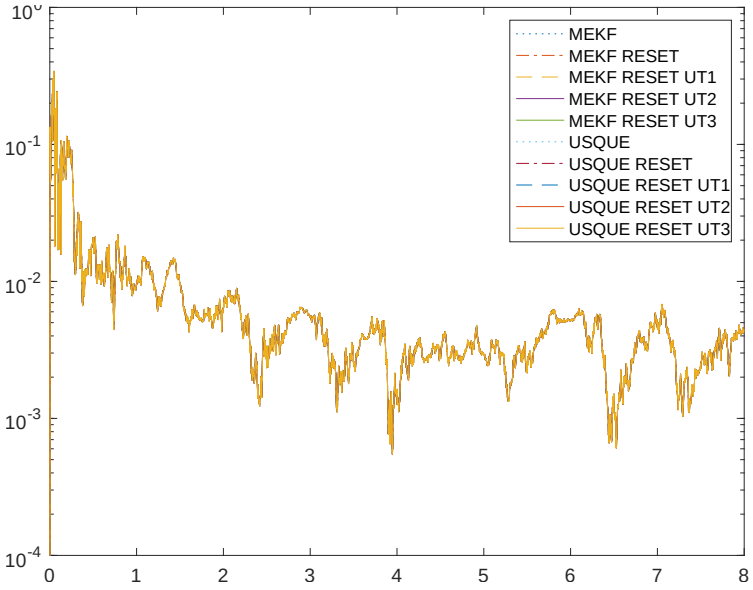

Fig. 2 Norm of attitude errors: case 1.

Table 1 Root mean square errors (deg): case 1

Algorithm	[0h, 8h]	[4h, 8h]
MEKF	0.0229	0.0036
MEKF RESET	0.0228	0.0036
MEKF RESET UT1	0.0228	0.0036
MEKF RESET UT2	0.0228	0.0036
MEKF RESET UT3	0.0228	0.0036
USQUE	0.0229	0.0036
USQUE RESET	0.0228	0.0036
USQUE RESET UT1	0.0228	0.0036
USQUE RESET UT2	0.0228	0.0036
USQUE RESET UT3	0.0228	0.0036

get so close together as to obscure one another. In Case 3, the second-order error-covariance resets are able to prevent the MEKF from diverging. They also improve USQUE, albeit not as significantly. In Cases 2 and 3, neither the MEKFs nor USQUEs with second-order resets are able to reduce the RMSE over the last four hours to 0.0036 deg. This indicates that the two cases are arduous ones, even for a second-order filter with a second-order reset.

The results in Fig. 5 and Table 4 show the average performances of the filters over 100 runs. They corroborate that second-order resets can greatly improve the estimation accuracy. Thanks to the less dramatic initial attitude errors, USQUE with a second-order reset converges to the same level of accuracy as in Case 1. It is interesting to note that USQUE with the first-order reset yields larger RMSEs than USQUE without reset. That indicates that in the presence of large attitude errors, the first-order reset does not always improve the performances of the filter.

When it comes to which second-order reset is the best, the evidence is not strong enough to be conclusive. In

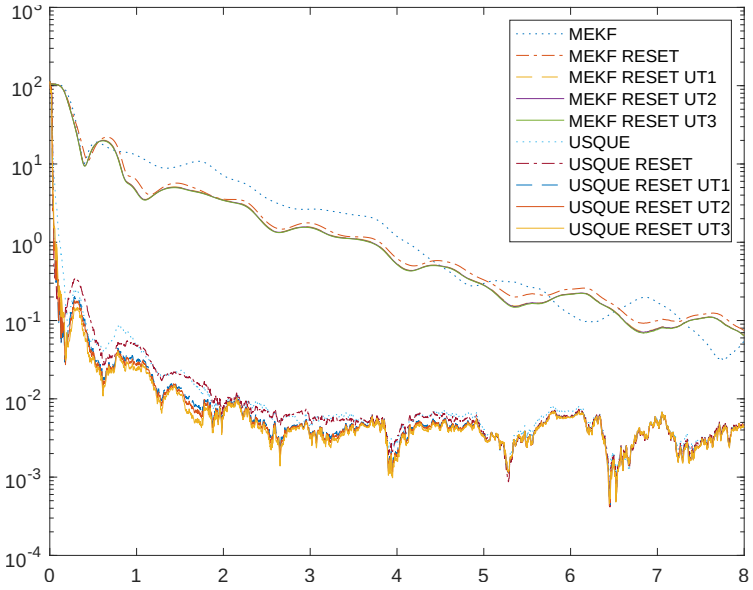

Fig. 3 Norm of attitude errors: case 2.

Table 2 Root mean square errors (deg): case 2

Algorithm	[0h, 8h]	[4h, 8h]
MEKF	18.3713	0.3546
MEKF RESET	17.3939	0.3001
MEKF RESET UT1	16.9163	0.2571
MEKF RESET UT2	16.8778	0.2554
MEKF RESET UT3	16.8409	0.2525
USQUE	4.9477	0.0049
USQUE RESET	5.4267	0.0045
USQUE RESET UT1	5.3007	0.0041
USQUE RESET UT2	5.2510	0.0041
USQUE RESET UT3	5.0080	0.0040

general, the difference between $\hat{\boldsymbol{\delta}}^*$ and $\hat{\boldsymbol{\delta}}$ is large only during the transient phase of the filter, but it is unclear whether, during that phase, the Gaussian assumption, made by the UT, is always valid and the UT always sufficiently accurate. What is not ambiguous is that the first second-order reset is the simplest and fastest.

B. Linear Measurement Model and Linear Error-Covariance Reset in Case 3

Case 3 is revisited in this test. In Case 3, the divergence of the MEKF without the error-covariance reset ("MEKF") or with the linear error-covariance reset ("MEKF RESET") is most likely caused by large updates based on the linearization of the nonlinear measurement model. Now, the linear measurement model given by Eq. (98) is used in Case 3. Note that this measurement model is linear in the Rodrigues-Gibbs vector $\boldsymbol{g}$, but not in the other attitude parameterizations. Six new MEKFs that estimate $\hat{\boldsymbol{g}}$ based on the linear measurement model are included in the test. The new MEKF without

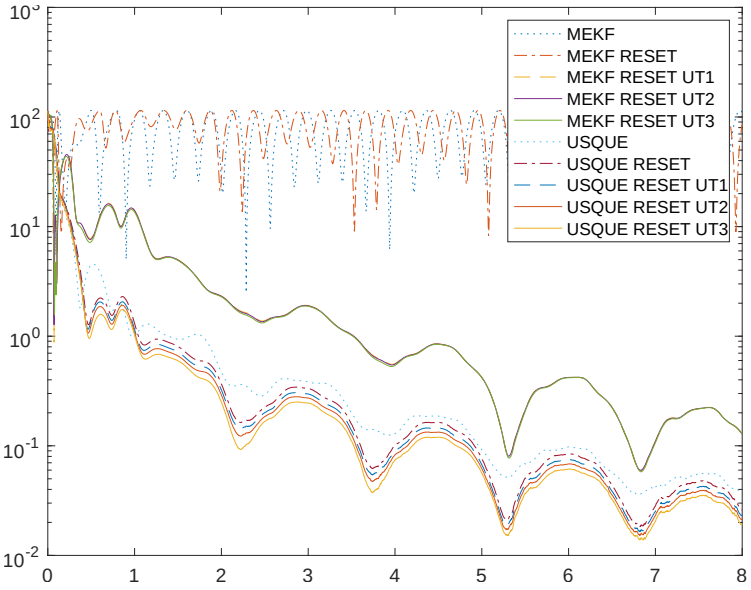

Fig. 4 Norm of attitude errors: case 3.

Table 3 Root mean square errors (deg): case 3

Algorithm	[0h, 8h]	[4h, 8h]
MEKF	81.8154	83.3004
MEKF RESET	84.9284	82.7957
MEKF RESET UT1	11.0993	0.4141
MEKF RESET UT2	11.0800	0.4133
MEKF RESET UT3	10.9959	0.4104
USQUE	9.4079	0.0999
USQUE RESET	9.1443	0.0819
USQUE RESET UT1	9.1939	0.0727
USQUE RESET UT2	9.0591	0.0667
USQUE RESET UT3	8.6668	0.0598

error-covariance reset is labeled "MEKF LIN." All the other new MEKFs using linear error-covariance resets are labeled "MEKF LIN RESET," followed by the specific Γ matrix used. To compute $\Gamma_\delta(\hat{\boldsymbol{\delta}})$, where $\hat{\boldsymbol{\delta}} \neq \hat{\boldsymbol{g}}$, $\hat{\boldsymbol{g}}$ is converted to $\hat{\boldsymbol{\delta}}$ first. With the linear measurement model, a second-order measurement update or second-order error-covariance reset is not needed. Therefore, USQUE and filters with second-order error-covariance resets are not included.

The results are summarized in Fig. 6 and Table 5. For comparison purposes, the MEKFs that diverge ("MEKF" and "MEKF RESET") are included as well. Using the linear measurement model, all the new MEKFs converge. The slow convergence of the MEKF without the error-covariance reset clearly shows the necessity of the error-covariance reset. All but the MEKF with $\Gamma_g(\hat{\boldsymbol{g}})$ converge fast to the same level of attitude errors as those in Case 1. They work equally well. The matrix $\Gamma_g(\hat{\boldsymbol{g}})$ leads to large errors in the two test cases in Section VII too. Figure 7 shows the attitude errors around the x-axis (roll errors) in a single run with their respected 3σ bounds for the MEKF LIN RESET using Γ'_g

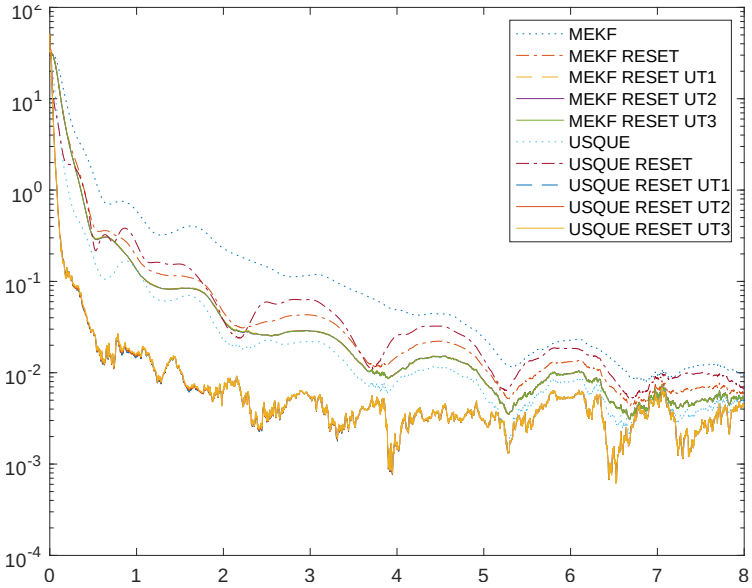

Fig. 5 Root mean square of norm of attitude errors over 100 runs: case 4.

Table 4 Root mean square errors (deg): case 4

Algorithm	[0h, 8h]	[4h, 8h]
MEKF	3.8324	0.0242
MEKF RESET	3.2393	0.0121
MEKF RESET UT1	3.2548	0.0086
MEKF RESET UT2	3.2392	0.0086
MEKF RESET UT3	3.2496	0.0085
USQUE	2.2848	0.0066
USQUE RESET	2.1611	0.0172
USQUE RESET UT1	1.8960	0.0037
USQUE RESET UT2	1.8949	0.0037
USQUE RESET UT3	1.9070	0.0037

and MEKF LIN. Similar characteristics are shown in the other axes. It is clearly seen that the reset operation results in consistent estimates with their respective 3σ bounds throughout the entire time span, while without the reset the estimates are not consistent with their respective 3σ bounds.

Conclusion

Although the multiplicative extended Kalman filter (MEKF) always requires a global attitude reset step immediately after a measurement update, it usually does not include the associated error-covariance reset. To understand the effects of the error-covariance reset on the MEKF, analytical expressions for the post-reset error-covariance were derived for the Gibbs vector, the vector part of the quaternion, the modified Rodrigues parameter vector, and the rotation vector. It is concluded through analytical analyses that in addition to the global attitude, the error-covariance should also be

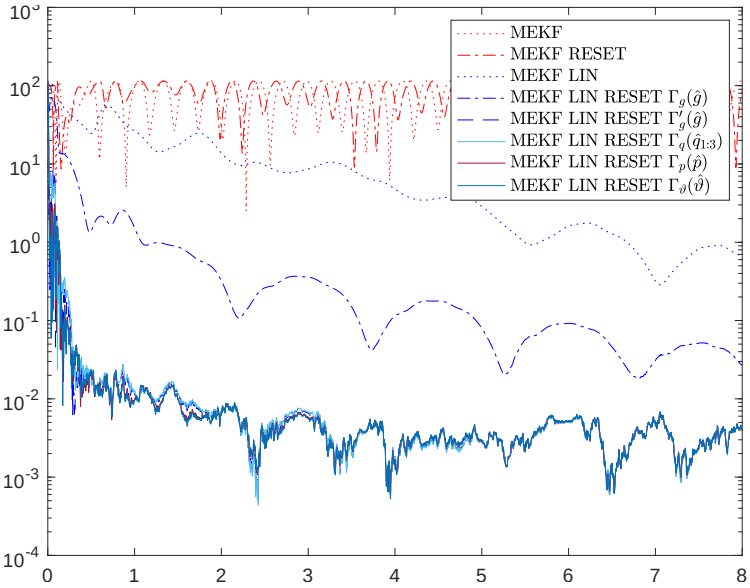

Fig. 6 Norm of attitude errors with linear measurement model: case 3.

Table 5 Root mean square errors (deg) with linear measurement model: case 3

Algorithm	[0h, 8h]	[4h, 8h]
MEKF	81.8154	83.3004
MEKF RESET	84.9284	82.7957
MEKF LIN	19.9444	2.1524
MEKF LIN RESET $\Gamma_g(\hat{\boldsymbol{g}})$	7.7097	0.0889
MEKF LIN RESET $\Gamma'_g(\hat{\boldsymbol{g}})$	2.9673	0.0035
MEKF LIN RESET $\Gamma_q(\hat{\boldsymbol{q}})$	3.7930	0.0034
MEKF LIN RESET $\Gamma_p(\hat{\boldsymbol{p}})$	3.2400	0.0035
MEKF LIN RESET $\Gamma_\vartheta(\hat{\boldsymbol{\vartheta}})$	3.3381	0.0035

reset. Theoretically, the error-covariance reset is a second-order operation though. Performance comparisons through numerical simulations showed that, in the presence of large estimation updates, the first-order error-covariance reset did not necessarily improve the accuracy or convergence properties of the MEKF or the Unscented filter. But, the second-order error-covariance reset may have benefits for both filters. Both results are most likely due to the fact that the error-covariance reset is a second-order effect, which may provide better performance characteristics for higher-order filters such as the Unscented filter. The linear measurement model can significantly improve the convergence properties of the MEKF, but the error-covariance reset is still needed when the attitude updates are large.

Acknowledgments

The authors would like to thank J. Russell Carpenter from NASA Goddard Space Flight Center for several useful comments.

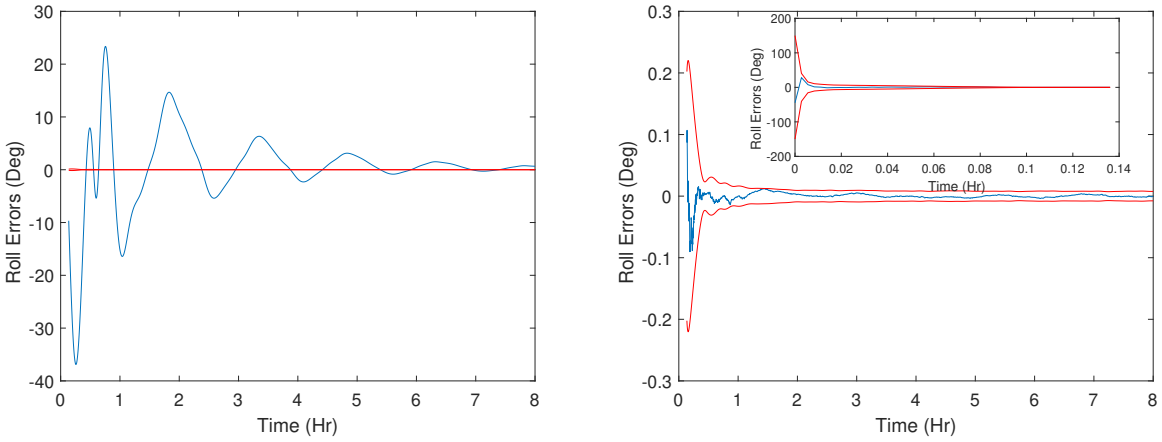

(a) MEKF LIN **(b) MEKF LIN RESET**

Fig. 7 Comparison of roll errors and their respective 3σ bounds.

References

[1] Crassidis, J. L., Markley, F. L., and Cheng, Y., "Survey of Nonlinear Attitude Estimation Methods," *Journal of Guidance, Control, and Dynamics*, Vol. 31, No. 1, 2007, pp. 12–28. doi:10.2514/1.22452.

[2] Savage, P. G., "Blazing Gyros: The Evolution of Strapdown Inertial Navigation Technology for Aircraft," *Journal of Guidance, Control, and Dynamics*, Vol. 36, No. 3, 2013, pp. 637–655. doi:10.2514/1.60211.

[3] Crassidis, J. L., and Junkins, J. L., *Optimal Estimation of Dynamic Systems*, 2nd ed., Chapman & Hall/CRC, Boca Raton, FL, 2012, Chap. 3, p. 703.

[4] Stuelpnagel, J., "On the Parameterization of the Three-Dimensional Rotation Group," *SIAM Review*, Vol. 6, No. 4, 1964, pp. 422–430.

[5] Lefferts, E. J., Markley, F. L., and Shuster, M. D., "Kalman Filtering for Spacecraft Attitude Estimation," *Journal of Guidance, Control, and Dynamics*, Vol. 5, No. 5, 1982, pp. 417–429. doi:10.2514/3.56190.

[6] Markley, F. L., "Attitude Error Representations for Kalman Filtering," *Journal of Guidance, Control, and Dynamics*, Vol. 63, No. 2, 2003, pp. 311–317. doi:10.2514/2.5048.

[7] Shuster, M. D., "Constraint in Attitude Estimation Part I: Constrained Estimation," *Journal of the Astronautical Sciences*, Vol. 51, No. 1, 2003, pp. 51–74. doi:10.1007/BF03546315.

[8] Shuster, M. D., "Constraint in Attitude Estimation Part II: Unconstrained Estimation," *Journal of the Astronautical Sciences*, Vol. 51, No. 1, 2003, pp. 75–101. doi:10.1007/BF03546316.

[9] Markley, F. L., "Attitude Estimation or Quaternion Estimation?" *Journal of the Astronautical Sciences*, Vol. 52, No. 1/2, 2004, pp. 221–238. doi:10.1007/BF03546430.

[10] Murrell, J. W., "Precision Attitude Determination for Multimission Spacecraft," *AIAA Guidance and Control Conference*, American Institute of Aeronautics and Astronautics, Reston, VA, 1978. doi:10.2514/6.1978-1248.

[11] Shuster, M. D., "A Survey of Attitude Representations," *Journal of the Astronautical Sciences*, Vol. 41, No. 4, 1993, pp. 439–517.

[12] Markley, F. L., and Crassidis, J. L., *Fundamentals of Spacecraft Attitude Determination and Control*, Springer, New York, NY, 2014, Chaps. 2, 6. doi:10.1007/978-1-4939-0802-8.

[13] Reynolds, R. G., "Asymptotically Optimal Attitude Filtering with Guaranteed Convergence," *Journal of Guidance, Control, and Dynamics*, Vol. 30, No. 1, 2008, pp. 114–122. doi:10.2514/1.30381.

[14] Markley, F. L., "Lessons Learned," *The Journal of the Astronautical Sciences*, Vol. 57, No. 1 & 2, 2009, pp. 3–29. doi:10.1007/BF03321491.

[15] Zanetti, R., Majji, M., Bishop, R. H., and Mortari, D., "Norm-Constrained Kalman Filtering," *Journal of Guidance, Control, and Dynamics*, Vol. 32, No. 5, 2009, pp. 1458–1465. doi:10.2514/1.43119.

[16] Mueller, M. W., Hehn, M., and D'Andrea, R., "Covariance Correction Step for Kalman Filtering with an Attitude," *Journal of Guidance, Control, and Dynamics*, Vol. 40, No. 9, 2017, pp. 2301–2306. doi:10.2514/1.G000848.

[17] Gill, R., Mueller, M. W., and D'Andrea, R., "Full-Order Solution to the Attitude Reset Problem for Kalman Filtering of Attitudes," *Journal of Guidance, Control, and Dynamics*, Vol. 43, No. 7, 2020, pp. 1232–1246. doi:10.2514/1.G004134.

[18] Psiaki, M. L., Theiler, J., Bloch, J., Ryan, S., Dill, R. W., and Warner, R. E., "ALEXIS Spacecraft Attitude Reconstruction with Thermal/Flexible Motions Due to Launch Damage," *Journal of Guidance, Control, and Dynamics*, Vol. 20, No. 5, 1997, pp. 1033–1041. doi:10.2514/2.4151.

[19] Gelb, A. (ed.), *Applied Optimal Estimation*, The MIT Press, Cambridge, MA, 1974, pp. 190–191.

[20] Shuster, M. D., "Kalman Filtering of Spacecraft Attitude and the QUEST Model," *Journal of the Astronautical Sciences*, Vol. 38, No. 3, 1990, pp. 377–393.

[21] Wan, E., and van der Merwe, R., "The Unscented Kalman Filter," *Kalman Filtering and Neural Networks*, edited by S. Haykin, John Wiley & Sons, New York, NY, 2001, Chap. 7.

[22] Crassidis, J. L., and Markley, F. L., "Unscented Filtering for Spacecraft Attitude Estimation," *Journal of Guidance, Control, and Dynamics*, Vol. 26, No. 4, 2003, pp. 536–542. doi:10.2514/2.5102.

[23] Chang, L., Hu, B., and Li, K., "Iterated Multiplicative Extended Kalman Filter for Attitude Estimation Using Vector Observations," *IEEE Transactions on Aerospace and Electronic Systems*, Vol. 52, No. 4, 2016, pp. 2053–2060. doi:10.1109/TAES.2016.150237.

[24] Cheng, Y., and Crassidis, J. L., "Particle Filtering for Attitude Estimation Using a Minimal Local-Error Representation," *Journal of Guidance, Control, and Dynamics*, Vol. 33, No. 4, 2010, pp. 1305–1310. doi:10.2514/1.47236.

[25] Arulampalam, M. S., Maskell, S., Gordon, N., and Clapp, T., "A Tutorial on Particle Filters for Online Nonlinear/Non-Gaussian Bayesian Tracking," *IEEE Transactions on Signal Processing*, Vol. 50, No. 2, 2002, pp. 174–188. doi:10.1109/78.978374.

[26] Gustafsson, F., and Hendeby, G., "Some Relations Between Extended and Unscented Kalman Filters," *IEEE Transactions on Signal Processing*, Vol. 60, No. 2, 2012, pp. 545–555. doi:10.1109/TSP.2011.2172431.